Nuclear Science
NEA/NSC/DOC(2006)5

ISBN 92-64-02295-3

VVER-1000 Coolant Transient Benchmark

Phase 1 (V1000CT-1)
Vol. 2: Summary Results of Exercise 1
Point Kinetics Plant Simulation

Boyan D. Ivanov and Kostadin N. Ivanov
Nuclear Engineering Program
The Pennsylvania State University

NEA No. 6219

NUCLEAR ENERGY AGENCY
ORGANISATION FOR ECONOMIC CO-OPERATION AND DEVELOPMENT

ORGANISATION FOR ECONOMIC CO-OPERATION AND DEVELOPMENT

The OECD is a unique forum where the governments of 30 democracies work together to address the economic, social and environmental challenges of globalisation. The OECD is also at the forefront of efforts to understand and to help governments respond to new developments and concerns, such as corporate governance, the information economy and the challenges of an ageing population. The Organisation provides a setting where governments can compare policy experiences, seek answers to common problems, identify good practice and work to co-ordinate domestic and international policies.

The OECD member countries are: Australia, Austria, Belgium, Canada, the Czech Republic, Denmark, Finland, France, Germany, Greece, Hungary, Iceland, Ireland, Italy, Japan, Korea, Luxembourg, Mexico, the Netherlands, New Zealand, Norway, Poland, Portugal, the Slovak Republic, Spain, Sweden, Switzerland, Turkey, the United Kingdom and the United States. The Commission of the European Communities takes part in the work of the OECD.

OECD Publishing disseminates widely the results of the Organisation's statistics gathering and research on economic, social and environmental issues, as well as the conventions, guidelines and standards agreed by its members.

* * *

This work is published on the responsibility of the Secretary-General of the OECD. The opinions expressed and arguments employed herein do not necessarily reflect the official views of the Organisation or of the governments of its member countries.

NUCLEAR ENERGY AGENCY

The OECD Nuclear Energy Agency (NEA) was established on 1st February 1958 under the name of the OEEC European Nuclear Energy Agency. It received its present designation on 20th April 1972, when Japan became its first non-European full member. NEA membership today consists of 28 OECD member countries: Australia, Austria, Belgium, Canada, the Czech Republic, Denmark, Finland, France, Germany, Greece, Hungary, Iceland, Ireland, Italy, Japan, Luxembourg, Mexico, the Netherlands, Norway, Portugal, Republic of Korea, the Slovak Republic, Spain, Sweden, Switzerland, Turkey, the United Kingdom and the United States. The Commission of the European Communities also takes part in the work of the Agency.

The mission of the NEA is:

- to assist its member countries in maintaining and further developing, through international co-operation, the scientific, technological and legal bases required for a safe, environmentally friendly and economical use of nuclear energy for peaceful purposes, as well as
- to provide authoritative assessments and to forge common understandings on key issues, as input to government decisions on nuclear energy policy and to broader OECD policy analyses in areas such as energy and sustainable development.

Specific areas of competence of the NEA include safety and regulation of nuclear activities, radioactive waste management, radiological protection, nuclear science, economic and technical analyses of the nuclear fuel cycle, nuclear law and liability, and public information. The NEA Data Bank provides nuclear data and computer program services for participating countries.

In these and related tasks, the NEA works in close collaboration with the International Atomic Energy Agency in Vienna, with which it has a Co-operation Agreement, as well as with other international organisations in the nuclear field.

FOREWORD

Under United States Nuclear Regulatory Commission (NRC) sponsorship, the Nuclear Energy Agency (NEA) of the Organisation for Economic Co-operation and Development (OECD) finalised a PWR main steam line break (MSLB) benchmark against thermal-hydraulic/neutron kinetics codes. In parallel, and again under NEA and NRC auspices, a coupled-code benchmark was completed for a BWR turbine trip (TT) transient. Over the course of defining and co-ordinating the NEA/NRC PWR MSLB and BWR TT benchmarks, a systematic approach was established to validate best-estimate coupled codes. This approach employs a multi-level methodology that not only allows for a consistent and comprehensive validation process, but also contributes to determining additional requirements and preparing a basis for licensing application of the coupled calculations for a specific reactor type, for example in order to establish a safety expertise in analysing reactivity transients. Professional communities formed during these benchmark activities engendered in-depth discussions of different aspects of accessing neutron kinetics modelling for a given reactor, and ways to implement best-estimate methodologies for transient analysis using coupled codes. Such are the benefits of establishing international coupled standard problems for each type of reactor.

In the framework of the United States Department of Energy (DOE) International Nuclear Safety Program (INSP), a project was started with an overall objective to access computer codes used in the safety analysis of VVER power plants, specifically for their use in analysing reactivity transients in a VVER-1000 reactor. As a result, a coupled benchmark problem based on the Bulgarian Kozloduy nuclear power plant (NPP) data was developed for the purpose of assessing neutron kinetics modelling for a VVER-1000 reactor. The problem is being analysed with both point kinetics and three-dimensional kinetics models. Based on the experience accumulated in safety analyses of Western-type reactors (such as the PWR and BWR international standard benchmark problems cited above), it was proposed that the VVER-1000 benchmark be extended to an international standard problem. In June 2001, the NEA Nuclear Science Committee (NSC) endorsed the coupled VVER-1000 benchmark problem as an international standard problem for the validation of best-estimate safety codes for VVER applications.

During the Starter International VVER-1000 Benchmark Meeting, which took place in Dresden, Germany on 30 May 2002, it was proposed and accepted by the participants that the VVER-1000 benchmark be designated as the VVER-1000 Coolant Transient Benchmark (V1000CT) and consist of two phases. Phase I (V1000CT-1), led by Pennsylvania State University (PSU), is a main coolant pump (MCP) switching on transient while the three other MCPs are in operation. Phase II (V1000CT-2), led by the *Commissariat à l'énergie atomique* (CEA), includes calculation of coolant-mixing experiments and an MSLB analysis. In June 2002, the NEA Nuclear Science Committee approved the extension of the benchmark to two phases, as outlined above. Both PSU and the CEA are working in co-operation with the Institute for Nuclear Research and Nuclear Energy (INRNE) in Sofia, Bulgaria. The benchmark sponsors are the OECD Nuclear Energy Agency (NEA), the US DOE and the CEA. The Kozloduy nuclear power plant (KNPP) is providing technical support and the Atomic Energy Research[1] (AER) Working Group D is collaborating in the benchmark activities.

[1] The AER is an international association on VVER reactor physics and reactor safety.

The V1000CT-1 benchmark reports are being published by the NEA in four volumes. The first volume, published in 2002, provided the specification for the V1000CT-1 benchmark problem. The specification report was jointly prepared by PSU and the INRNE, in co-operation with leading specialists from the KNPP. The specification covers the three exercises of Phase I and the required output information is given for each exercise. In addition, a CD-ROM has been prepared with the transient boundary conditions, decay heat values as a function of time and cross-section libraries.

Volume II summarises the results for Exercise 1 of the benchmark and identifies the key parameters and important issues concerning the thermal-hydraulic system modelling of the simulated transient. Exercise 1 helped the participants to initialise and test their system code models for further use in Exercise 3 on coupled 3-D kinetics/system thermal-hydraulics simulations.

Readers are kindly invited to note that many of the figures in the report were prepared in colour. Colour versions are available on the NEA website at www.nea.fr/html/science/egrsltb/v1000ct/.

Acknowledgements

The authors would like to thank Drs. J. Roglans-Ribas, T. Taiwo, P. Pizzica and J. Ahrens from the Argonne National Laboratory (ANL), Prof. J. Aragones from *Universidad Politecnica Madrid* (UPM), a member of the NEA Nuclear Science Committee, and Prof. F. D'Auria of the University of Pisa (UPISA), a member of NEA Committee on the Safety of Nuclear Installations, whose support and encouragement in establishing and carrying out this benchmark were invaluable.

This report is the sum of many efforts, by the participants, the funding agencies and the staff of the US DOE, the CEA and the NEA. Special appreciation goes to the report reviewers: E. Royer (CEA), S. Kliem (FZR) and E. Popov (ORNL). Their comments and suggestions were very valuable and significantly improved the quality of this report.

The authors wish to express their sincere appreciation of the outstanding support offered by the KNPP personnel in providing the plant data and discussing the transient characteristics, as well as to E. Sartori, who not only provided efficient administration, organisation and valuable technical recommendations, but most importantly provided friendly counsel and advice.

The authors wish to make a special mention of the members of the AER Working Group D on VVER Dynamics and Safety, and its Chairman P. Siltanen in particular, for their active participation and excellent technical advice.

Finally, we are grateful to A. Costa for devoting her competence and skills to preparing this report for publication.

TABLE OF CONTENTS

List of tables

List of figures

LIST OF ABBREVIATIONS

ACAP	Automated Code Assessment Program
AER	Atomic energy research
ANL	Argonne National Laboratory
BC	Boundary condition
BOC	Beginning of cycle
BWR	Boiling water reactor
CEA	Commissariat à l'Énergie Atomique
CT	Coolant transient
DOE	Department of Energy
DTC	Doppler temperature coefficient
EFPD	Effective full power days
EHRS	Electro-hydraulic regulative system
EHTC	Electro-hydraulic turbine controller
FA	Fuel assembly
FOM	Figure of merit
FWP	Feedwater pump
FZK	Forschungszentrum Karlsruhe
FZR	Forschungszentrum Rossendorf
GRS	Gesellschaft für Anlagen- und Reaktorsicherheit
HP	Hot power
HZP	Hot zero power
INRNE	Institute for Nuclear Research and Nuclear Energy
INSP	International Nuclear Safety Program
KI	Kurchatov Institute
KNPP	Kozloduy nuclear power plant
KU	Kiev University
LWR	Light water reactor
MCP	Main coolant pump
ME	Mean error
MSE	Mean square error
MSLB	Main steam line break
MTC	Moderator temperature coefficient
NEA	Nuclear Energy Agency
NFMS	Neutron flux monitoring system (in-core reactor control system)

NPP	Nuclear power plant
NRC	Nuclear Regulatory Commission
NRI	Nuclear Research Institute
NSC	Nuclear Science Committee
OECD	Organisation for Economic Co-operation and Development
ORNL	Oak Ridge National Laboratory
PSU	Pennsylvania State University
PWR	Pressurised water reactor
RCS	Reactor coolant system
RPC	Reactor power controller
RPLC	Reactor power limitation controller
SDRS	Soviet-designed Reactor Safety
SG	Steam generator
TG	Turbo generator
TT	Turbine trip
UES	Universal electronic system
UPISA	University of Pisa
UPM	Universidad Politecnica Madrid
V1000CT	VVER-1000 Coolant Transient
VE	Variance of error
VTT	Valtion Teknillinen Tutkimuskeskus
VVER	Water water power reactor

Chapter 1

INTRODUCTION

In the recent past, the analysis of plant transients and the analysis of reactor core behaviour were performed separately. Usually, the core was represented by a point kinetics model to analyse plant transients and, for the core physics calculations, boundary conditions were imposed at the inlet and the outlet of the core. In reality, these boundary conditions depend on the power generation in the core. To ensure a realistic description of the physical phenomena in an accident analysis, the application of coupled codes is required. In recent years code developers began coupling three-dimensional (3-D) neutron kinetics codes with advanced thermal-hydraulics system codes. Such complex computer codes allow modelling of the entire reactor system, including a 3-D neutronics core. When reactivity initiated accidents with an asymmetric neutron flux distribution in the core are analysed, only such coupled codes are capable of estimating the real feedback effects. These codes can perform safety analyses in order to replace the conservative estimations with best-estimate calculations.

The US Department of Energy (DOE) has established a national laboratory team to support the planning, management and implementation of its Soviet-designed Reactor Safety Program (SDRS). One of the goals of this programme is to develop models for VVER reactors for use in coupled thermal-hydraulics/neutron kinetics codes for the analysis of specific transients. The specific technical goals of the project were:

- development of the methodology for performing coupled thermal-hydraulics/neutron kinetics multi-dimensional analyses of VVER reactors;

- development and analysis of benchmark problems to determine applicability of the 3-D coupled thermal-hydraulics/neutron kinetics codes to safety analysis of VVER special transients.

As a result, a benchmark problem has been established in order to determine applicability of the coupled codes to safety analysis of VVER special transients [1]. A small benchmark team at Pennsylvania State University (PSU) was responsible for authoring the VVER-1000 benchmark specification using Bulgarian Kozloduy NPP (KNPP) data. Based on the experience of the PSU team accumulated in safety analyses of the Western-type reactors (Pressurised Water Reactor (PWR) Main Steam Line Break (MSLB) [2] and Boiling Water Reactor (BWR) Turbine Trip (TT) [3]) it was proposed that the VVER-1000 benchmark problem be extended to an international standard problem. At its topical meeting in Paris in June 2001, the NEA Nuclear Science Committee (NSC) approved and endorsed the developed coupled VVER-1000 benchmark problem as an international standard problem for validation of the best-estimate safety codes for VVER applications; it was designated as the V1000CT benchmark. The benchmark specification for Phase I [4] was prepared jointly by PSU and the Institute for Nuclear Research and Nuclear Energy (INRNE) in co-operation with leading specialists from the KNPP. The reference problem chosen for simulation in a VVER-1000 is a main coolant pump (MCP) switching on while the other three main coolant pumps are in operation. It is an experiment that was conducted as part of the start-up tests by Bulgarian and Russian engineers during the plant-commissioning phase at KNPP Unit #6. The test was done as it is important for the safety of

the NPP. This event is characterised by a rapid increase in the flow through the core resulting in a coolant temperature decrease, which is spatially dependent. The V1000CT-1 benchmark has three main goals:

- to verify the capability of system codes to analyse complex transients with coupled core/plant interactions;
- to fully test the 3-D neutronics/thermal-hydraulic coupling;
- to evaluate discrepancies between predictions of coupled codes in best-estimate transient simulations (code-to-code comparative analysis) and between coupled code predictions and plant data (code-to-data comparative analysis).

The three exercises, discussed below, fulfil the goals of this benchmark phase.

Exercise 1 – Point kinetics plant simulation

The purpose of this exercise is to test the primary and secondary system model responses using a point kinetics approximation. The benchmark specification provides all the necessary point kinetics data. Using this exercise, participants can verify and initialise their system models and they can eliminate all the problems emerging from user modelling, which later could be helpful for the best-estimate comparisons.

Exercise 2 – Coupled 3-D neutronics/core thermal-hydraulics response evaluation

The purpose of this exercise is to model the core and the reactor vessel only. The benchmark provides inlet and outlet core transient boundary conditions. Using this exercise the participants can verify and initialise their core models, the coupling schemes and the cross-section library utilisation.

Exercise 3 – Best-estimate coupled-code plant transient modelling

The first two exercises are preparation for the third exercise, which combines elements of the first two. In this exercise the participants must analyse the entire transient.

This report summarises the comparative analyses of the submitted results for Exercise 1. In total, 10 results were submitted by participants representing 9 organisations from 7 countries. Table 1.1 shows the list of the participants in Exercise 1 together with the names of the codes used for simulation of Exercise 1.

Chapter 2 describes Exercise 1, including the initial conditions. Chapter 3 discusses the comparative statistical methodology used for integral parameters, and time histories. Chapter 4 is a comparative analysis of the final results of Exercise 1, while Chapter 5 is a summary of the conclusions drawn from the analysis of Exercise 1.

Table 1.1. List of participants in Exercise 1

Participant no.	Name	Country	Code
1	FZK	Germany	RELAP5/MOD3.3
2	GRS	Germany	ATHLET
3	INRNE-1[1]	Bulgaria	RELAP5/MOD3.2
4	INRNE-2[2]	Bulgaria	CATHARE2 V1.3
5	KI	Russia	ATHLET 2.0A
6	KU	Ukraine	RELAP5-3D
7	NRI	Czech Republic	ATHLET Mod 2.0 Cycle A
8	ORNL	USA	RELAP5-3D
9	PSU	USA	TRAC-PF1/MOD2
10	UPISA	Italy	RELAP5/MOD3.3

[1] Pavlin Groudev's team.
[2] Nikolay Kolev's team.

Chapter 2

DESCRIPTION OF EXERCISE 1

2.1 Introduction

During the plant-commissioning of the Kozloduy NPP Unit #6, a number of experiments were performed. One of the experiments was an investigation of the behaviour of the nuclear power reactor parameters in the case of one MCP switching on while the other three main coolant pumps are in operation. The purpose of the experiment was a complete testing of the reliability of the entire power plant equipment.

Before the experiment, the reactor power level was reduced from 75% of the nominal level (2 250 MW) to approximately 21% by the consecutive switching-off of MCP#2 and MCP#3. A few hours before the experiment MCP #2 was switched back on, and the power was stabilised at 30% in accordance with the technical specification requirements for Units #5 and #6 (both VVER-1000), which specify that switching on one main coolant pump in operation should be performed when the reactor power is at 30% of the nominal level.

The reactor power controller (RPC) is a part of the unit power control system and operates in co-ordination with the reactor power limitation controller (RPLC) and the electro-hydraulic turbine controller (EHTC). The controller stabilises the reactor power or forces the reactor to follow the turbine power. The RPC does not establish any set-point specification devices and stores the current values of neutron power or main steam header pressure as a set-point at the time of switching on. In order to reset a set-point, switching off and then switching on to the appropriate mode is necessary. The controller uses the control rod group #10 to operate. During the particular transient used for this benchmark the control rod group #10 does not change position.

The RPLC constrains the maximum thermal and neutron power within limits automatically chosen depending on the operational status of certain plant components, such as MCP, feedwater pump (FWP), steam generator (SG) and turbo generator (TG). The RPLC inserts the control rod group #10 with a normal operation speed of 2 cm/sec. A control signal is the neutron flux, measured by the neutron flux monitoring system (NFMS). This signal is corrected once every 50 seconds using the thermal power evaluated on the basis of the average temperature rise in the operating loops.

Depending on the initiating event, the reactor power is lowered to and then kept at specified set-points by RPLC as follows:

- 1 out of 4 MCPs trip: to 67%N_n;
- 2 out of 4 diametrically placed MCPs trip out of 4: to 50%N_n;
- 2 out of 4 neighbouring MCPs trip out of 4: to 40%N_n.

During the experiment of switching on MCP #3, the system and equipment of Unit #6 performed according to the design requirements for the corresponding level of the reactor power. Design equipment registers and records the parameters in case of a transient event. The design equipment includes the universal electronic system (UES) and the in-core neutron flux monitoring system (NFMS).

At the beginning of the transient the initial power level is about 30% of the nominal with control rod group #10 withdrawn 36% from the reactor core. Analysis of the initial 3-D relative power distribution showed that this insertion introduced axial neutronic asymmetry in the core. At the beginning of the transient a thermal-hydraulic asymmetry is observed coming from the colder water introduced in one-quarter of the core when MCP #3 is switched on. This causes a spatial asymmetry in the reactivity feedback, which has been propagated through the transient and combined with the insertion of positive reactivity.

2.2 Initial steady-state conditions

The reactor is at beginning of cycle (BOC) with an average core exposure of 30.7 EFPD (effective full power days) and a soluble boron concentration of 5.95 g/kgH_2O. At the beginning of the experiment three pumps are in operation: #1, #2 and #4, and the reactor power is at 29.45% nominal power according to the equipment that controls neutron flux. MCP #1, #2 and #4 are working under stable conditions and MCP #3 is out of operation. Table 2.1 lists the initial conditions. The inlet temperature in the reactor core is about 555.00 K. The temperature differences between the hot and cold legs for the loops with working MCP vary between 8.3 and 11.5 K, while the same temperature difference for loop #3 with the MCP out of operation is -3.6 K. The total mass flow through the core is about 13 611 kg/s with an average flow of 5 000 kg/s through each of the working loops and negative (reverse) flow of -1 544 kg/s in loop #3. The electro-hydraulic regulative system (EHRS) supports the pressure in the main steam collector when the turbine generator works at 164.0 ± 10 MW. All regulators are in automatic regime. Table 2.2 defines the initial steady states. The above-described initial conditions of the transient are referred to as hot power (HP) conditions. Additionally, a hot zero power (HZP) state was defined for initialisation of the 3-D core neutronics model for the second exercise.

In order to render the simulation compatible we must specify point kinetics model inputs, which preserve axial and radial core power distributions obtained with the 3-D neutronics model. The following parameters for the point kinetics model and the 3-D neutronic transient core model should be consistent:

- control rod group #10 worth;
- radial power distribution;
- axial power distribution;
- moderator temperature coefficient;
- Doppler temperature coefficient.

All other initial and boundary conditions must also be identical for the two models. Table 2.3 lists a summary of the input values for the point kinetics input. HP radial and axial relative power distributions (based on 10 equal nodes of 35.5 cm axial height) are shown in Figures 2.1 and 2.2, respectively.

Table 2.1. Initial conditions for KNPP Unit #6 at 883.5 MWt

Parameter	Value
Core power, MWt	824.00
Primary side pressure, MPa	15.6
RCS first cold leg temperature, K	555.55
RCS second cold leg temperature, K	554.55
RCS third cold leg temperature, K	554.35
RCS fourth cold leg temperature, K	555.25
RCS first hot leg temperature, K	567.05
RCS second hot leg temperature, K	562.85
RCS third hot leg temperature, K	550.75
RCS fourth hot leg temperature, K	566.15
Core flow rate, kg/s	13 611
First loop flow rate, kg/s	5 031
Second loop flow rate, kg/s	5 069
Third loop flow rate, kg/s	-1 544
Fourth loop flow rate, kg/s	5 075
Pressuriser level, m	7.44
Water level in SG1, m	2.30
Water level in SG2, m	2.41
Water level in SG3, m	2.49
Water level in SG4, m	2.43
Secondary side pressure, MPa	5.937

Table 2.2. Definition of steady states

Number	T-H conditions	Control rod positions
0	HZP	Groups 1-8 ARO[1] Group 9 36% inserted Groups 10 ARI[2]
1	HP	Groups 1-9 ARO Group 10 is 36% withdrawn

[1] ARO – all rods out.
[2] ARI – all rods inserted.

Table 2.3. Summary of point kinetics analysis input values

Parameter	Value
HP MTC, %/K	-2.49E-03
HP DTC, %/K	-2.89E-03
HP delayed neutron fraction (β_{eff})	0.7268E-02
HP prompt neutron lifetime	0.267E-04
Control rod group #10 worth, %dk/k	0.61
Ejected rod worth, %dk/k	0.08
Tripped rod worth, %dk/k	7.02

Figure 2.1. Initial HP radial power distribution

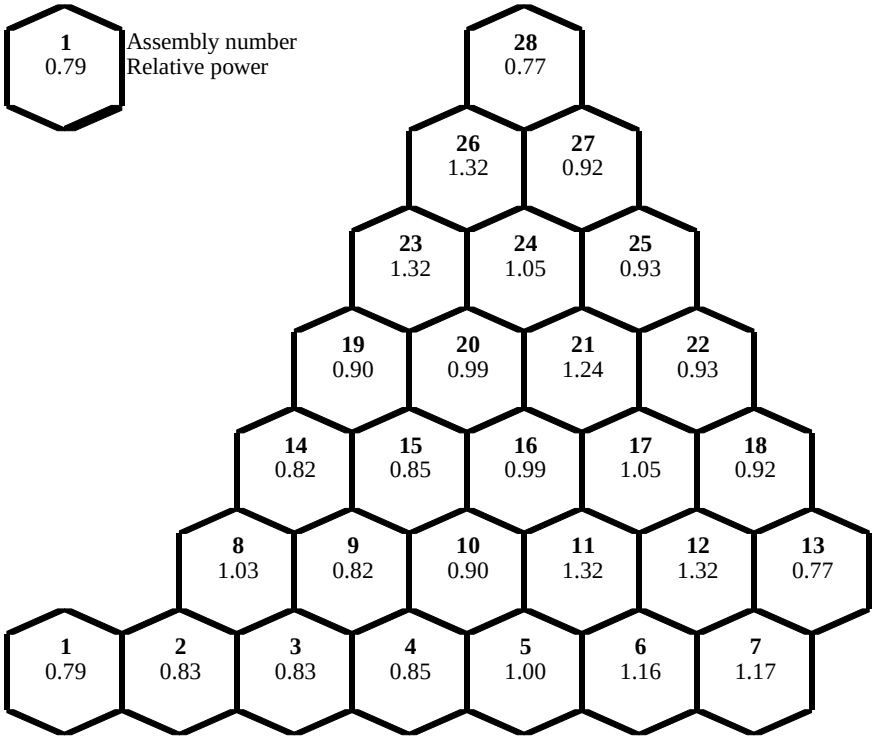

Figure 2.2. Initial HP core average axial relative power distribution

Bottom

0.34 0.69 0.94 1.10 1.20 1.30 1.38 1.36 1.11 0.59

Top

2.3 Transient calculations

The key assumptions for performing MCP transient analyses are summarised in Table 2.4. The transient test scenario is as follows:

1) At reactor power 27.46% N_{nom} MCP #3 is switched on.

2) After switching on MCP #3 the reactor power gradually increases to 29.8% N_{nom}.

3) Pressuriser water level decreases from 744 cm to 728 cm.

4) Water level in SG #3 decreases by 9 cm.

5) EHTC supports the pressure in MSH at a level of 6.0 ± 0.05 MPa when the TG power is 164.0 ± 10 MW.

6) The flow rate in loop #3 reverses back to normal at the 13^{th} second of the switching on of MCP #3. The timing is consistent with reactivity increase, as observed through the reactor power set-points.

During the transient, as a result of the switching on of MCP #3, there is an increased mass flow through the core. The cooling of the core is improved and re-distributed while the thermal core power level increases slightly (the total power increase during the transient is between 27.46% and 29.8% of the nominal level). The non-symmetric cooling of the reactor core results in non-symmetric reactivity feedback and subsequently non-symmetric radial power distribution.

At the end of the transient the temperature difference between hot and cold legs of loops #1, #2, and #4 slightly decreases:

- loop #1 – from 11.5 K to 8.8 K;
- loop #2 – from 8.3 K to 8.4 K;
- loop #4 – from 10.9 K to 8.9 K;
- loop #3 – from -3.6 K to 8.2 K.

The most noticeable change is in the temperature difference for loop #3. This results in a dynamically changing spatial distribution of reactivity feedback during the transient and subsequently in a dynamically changing spatial power distribution.

Since the objective of this benchmark is not to examine pump models of different system codes, the boundary conditions of MCP #3 rotor speed are provided in Table 2.5.

Transient boundary conditions for feedwater flow and secondary side pressure for each SG are provided in Tables 2.6 and 2.7, respectively. Feedwater temperature during the transient is 437.0 K.

The logic of the pressuriser heaters during the transient is given in Table 2.8. Make-up and let-down systems work during the transient with a steady mass flow rate of 9.19 kg/s.

The neutronics and thermal-hydraulic information presented in Chapters 2 and 3 of the V1000CT-1 benchmark specification [4] is sufficient for the calculation of Exercise 1.

Table 2.4. KNPP analysis assumptions

Parameter	Value
Thermal power loop #1, MWt	278
Thermal power loop #2, MWt	231
Thermal power loop #3, MWt	34
Thermal power loop #4, MWt	280

Table 2.5. MCP #3 rotor speed boundary conditions

Time, s	MCP #3 rotor speed, rad/s
0	0
0.5	9.4732
1	19.9464
1.5	31.4196
2	41.8928
4	61.366
6	73.8392
8	83.3124
10	90.7856
11	94.3567
14	102.3032
15	104.1964
17	104.1964
18-129	104.1964

Table 2.6. Feedwater flow boundary conditions

Time, s	SG1 FW flow, kg/s	SG2 FW flow, kg/s	SG3 FW flow, kg/s	SG4 FW flow, kg/s
0	155.624	170.7111	13.6154	155.362
4	155.407	158.378	14.053	155.239
8	153.289	141.714	14.2234	154.096
12	164.448	225.112	4.27314	160.604
16	167.115	204.968	14.948	163.023
20	169.039	178.835	15.7816	164.004
24	168.173	162.814	19.6741	163.498
28	164.576	150.481	26.3972	161.854
32	161.86	139.129	30.9824	160.053
36	158.205	128.557	49.2579	157.671
40	154.204	125.524	71.7107	155.385
44	149.555	124.721	87.5974	153.143
48	145.487	123.51	98.7642	149.429
52	142.21	124.369	106.576	146.329
56	139.657	125.338	111.813	143.729
60	137.894	124.563	115.07	141.335
64	136.221	123.812	117.479	139.125
68	134.795	124.422	119.371	137.255
72	133.601	124.693	120.833	135.691
76	132.59	124.79	121.963	134.357
80	131.723	125.07	122.814	133.197
84	130.954	125.081	123.43	132.184
88	130.284	125.077	123.953	131.321
92	129.699	125.244	124.311	130.572
96	129.212	125.344	124.662	129.925
100	128.786	125.409	124.918	129.371
104	128.419	125.483	125.122	128.898
108	128.102	125.51	125.268	128.506
112	127.833	125.618	125.397	128.163
116	127.617	125.71	125.486	127.868
120	127.42	125.732	125.581	127.614
124	127.253	125.751	125.699	127.411
128	127.111	125.841	125.771	127.236
129	127.087	125.855	125.776	127.187

Table 2.7. Steam generators' pressure boundary conditions

Time, s	SG1 pressure, Pa	SG2 pressure, Pa	SG3 pressure, Pa	SG4 pressure, Pa
0	6.09141E+06	6.09231E+06	6.05465E+06	6.09254E+06
4	6.09005E+06	6.09068E+06	6.04962E+06	6.09124E+06
8	6.09277E+06	6.0941E+06	6.06253E+06	6.09375E+06
12	6.09989E+06	6.09878E+06	6.09698E+06	6.09993E+06
16	6.08386E+06	6.08218E+06	6.08846E+06	6.08383E+06
20	6.06502E+06	6.06322E+06	6.0721E+06	6.06525E+06
24	6.06749E+06	6.06662E+06	6.07461E+06	6.06771E+06
28	6.07324E+06	6.07323E+06	6.08046E+06	6.07365E+06
32	6.07338E+06	6.07426E+06	6.08057E+06	6.07403E+06
36	6.07351E+06	6.07498E+06	6.08052E+06	6.07419E+06
40	6.07401E+06	6.07565E+06	6.08056E+06	6.07466E+06
44	6.07375E+06	6.0753E+06	6.0793E+06	6.07432E+06
48	6.07364E+06	6.07509E+06	6.07802E+06	6.07417E+06
52	6.07388E+06	6.07516E+06	6.07732E+06	6.0744E+06
56	6.07445E+06	6.07555E+06	6.07716E+06	6.07497E+06
60	6.07482E+06	6.07586E+06	6.07703E+06	6.07537E+06
64	6.07492E+06	6.07591E+06	6.07676E+06	6.0755E+06
68	6.07492E+06	6.07582E+06	6.07649E+06	6.07552E+06
72	6.07495E+06	6.07577E+06	6.07632E+06	6.07557E+06
76	6.07503E+06	6.0758E+06	6.07626E+06	6.07568E+06
80	6.07513E+06	6.07584E+06	6.07623E+06	6.07579E+06
84	6.07521E+06	6.07588E+06	6.07622E+06	6.07588E+06
88	6.07528E+06	6.07591E+06	6.07621E+06	6.07596E+06
92	6.07533E+06	6.07592E+06	6.0762E+06	6.07602E+06
96	6.07537E+06	6.07594E+06	6.07619E+06	6.07607E+06
100	6.07541E+06	6.07595E+06	6.07618E+06	6.07612E+06
104	6.07544E+06	6.07596E+06	6.07618E+06	6.07616E+06
108	6.07547E+06	6.07597E+06	6.07619E+06	6.0762E+06
112	6.0755E+06	6.07598E+06	6.0762E+06	6.07623E+06
116	6.07553E+06	6.07599E+06	6.0762E+06	6.07626E+06
120	6.07555E+06	6.076E+06	6.07621E+06	6.07629E+06
124	6.07557E+06	6.07601E+06	6.07621E+06	6.07631E+06
128	6.07559E+06	6.07602E+06	6.07622E+06	6.07633E+06
129	6.07559E+06	6.07602E+06	6.07622E+06	6.07633E+06

Table 2.8. Pressuriser heaters logic

Heaters group no.	Condition	State
1	P < 15.60 MPa	On
2	P < 15.60 MPa	On
3	P < 15.30 MPa	On
4	P < 15.30 MPa	On
1	P > 15.78 MPa	Off
2	P > 15.60 MPa	Off
3	P > 15.50 MPa	Off
4	P > 15.50 MPa	Off

Chapter 3

STATISTICAL METHODOLOGY AND DATA PROCESSING

This chapter presents the statistical methodology used for the comparative analysis of the results for Exercise 1 of Phase I of the V1000CT benchmark. As mentioned earlier, ten sets of results were submitted to the benchmark team. These results consist of integral parameters and time histories. The time histories had to be processed in order to be compared. The following subsections describe the statistical methodology used for the analyses of the two types of results as well as the data processing.

3.1 Integral parameters

The integral parameters include all of the initial steady-state values. Since plant-measured data exist for all of the required integral parameters, the absolute deviation from plant-measured data has been calculated using the following formula:

$$e_i = x_i - x_M$$

where e_i is the absolute deviation of the participant's result from the measured data, x_i is each participant's result, and x_M is the plant-measured value.

The absolute deviation has been chosen as a statistical method for comparative analysis of the integral parameters due to the existence of plant-measured uncertainty values.

3.2 Time histories

Nineteen different sets of time histories for which plant-measured data exist, were submitted by the participants. The plant-measured data were used as a reference in the statistical processing described in the next subsection. Conversely, nine sets of time histories for which there are no plant-measured data were submitted. These results were used to aid the comparative analyses of the participants' results. The time histories are compared in plots and the figure-of-merit (FOM) was calculated using the Automated Code Assessment Program (ACAP) [5] for the sets with plant-measured data.

3.3 Automated Code Assessment Program (ACAP)

As mentioned above, the comparative analyses were performed for code-to-data comparisons using the standard statistical methodology with ACAP. ACAP is a tool developed to provide quantitative comparisons between nuclear reactor systems' code results and experimental measurements. This software was developed in PSU under a NRC contract for use in the TRACE code consolidation efforts. ACAP's capabilities are described as follows:

- draws upon a mathematical toolkit to compare experimental data and NRC code simulations;
- returns quantitative FOM associated with individual and suite comparisons;
- accommodates the multiple data types encountered in NRC environments;
- incorporates experimental uncertainty in the assessment;
- provides “event windowing” capability;
- accommodates inconsistencies between measured and computed independent variables (e.g. different time steps);
- provides a framework for automated, tunable weighting of component measures in the construction of overall FOM accuracy.

ACAP is a PC and UNIX station-based application that can be run interactively on PCs with Windows 95/98/NT, in batch mode on PCs as a WINDOWS console application, or in batch mode on UNIX stations as a command line executable.

The mean error (ME), the variance of error (VE), and the mean square error (MSE) methods, as well as their combination (normalised weight), were used for the FOM calculations for the time histories [5]. Figure 3.1 shows a snapshot of the FOM configuration in ACAP calculations for Exercise 1 of the benchmark. These methods are advanced techniques for analysis of time history data. The following equations represent the theory portion of these methods.

Figure 3.1. FOM configuration in ACAP

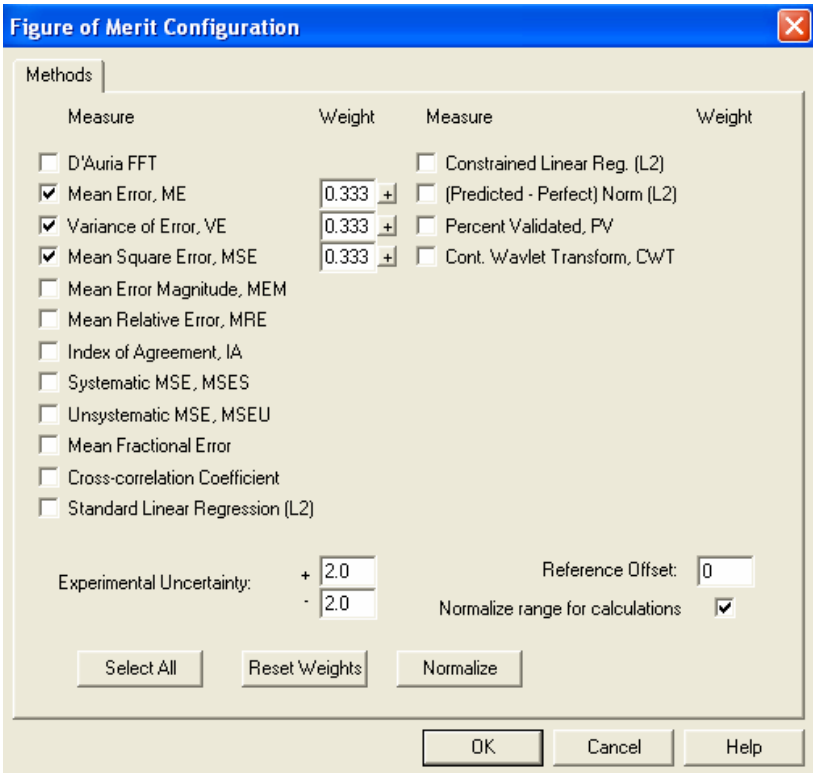

Mean error (ME)

$$ME = \frac{1}{N}\left\{\sum_{i=1}^{N}\left(O_i - P_i\right)\right\} \tag{3.1}$$

where N is the number of data values, i is the sample index, O_i is the i-th datum in the experimental set and P_i is the i-th datum in the computed set.

Variance of error (VE)

$$\sigma^2 = VE = \frac{1}{\left(N-1\right)}\left\{\sum_{i=1}^{N}\left(O_i - P_i - ME\right)^2\right\} \tag{3.2}$$

Mean square error (MSE)

$$MSE = \frac{1}{N}\left\{\sum_{i=1}^{N}\left(O_i - P_i\right)^2\right\} \tag{3.3}$$

The FOM equations for the three methods are outlined below:

$$FOM_{ME} = \frac{1}{\left(\left|ME\right| + 1\right)} \tag{3.4}$$

$$FOM_{VE} = \frac{1}{\left(VE + 1\right)} \tag{3.5}$$

$$FOM_{MSE} = \frac{1}{\left(MSE + 1\right)} \tag{3.6}$$

FOM indicates whether the participant results are closer to the reference solution. The FOM closer to unity indicates a better agreement.

3.4 Data processing

Participants' results for the time histories had to be processed in two different ways in order to be compared with each other and with the existing plant data.

First, in order to avoid the effects of participants' initialisation for steady state on the comparative analysis, the actual values of the time history data were set to zero and were designated *delta changes*. The delta changes were calculated subtracting the initial value (at time zero) from the rest of the values.

Second, the time histories for hot and cold leg coolant temperatures had to be altered so as to account for the time delay of the temperature measurement system. The thermo-couples and thermo-resistors in Kozloduy NPP are encapsulated in tubes which filter the measured signals. Their low pass filter characteristics can be described with the methodology developed in [6], described below.

The signal is proportional to:

$$S(t) = 0.05 \times S_f(t) + S_d(t) \tag{3.7}$$

where t is time and $S_f(t)$ is coolant temperature.

The delayed signal part in Eq. (3.7) is:

$$S_d(\bar{r},t) = \sum_j \lambda_j C_j(\bar{r},t) \tag{3.8}$$

where λ_j is the decay constant of delayed signal part j.

The time dependence of the delayed signal part in Eq. (3.8) is given by:

$$C_j(t) = \beta_j \int_{t_0}^{t} e^{-\lambda_j (t-t')} S_f(t') dt' + C_j(t_0) e^{-\lambda_j (t-t_0)} \tag{3.9}$$

where β_j is the fraction of delayed signal part j.

It is assumed that the temperature S_f varies linearly during a time step. A recurrence formula is obtained:

$$C_j^1 = C_j^0 e^{-\lambda_j \Delta t} + \beta_j \eta_j(\Delta t) S_f^0 + \beta_j \xi_j(\Delta t) S_f^1 \tag{3.10}$$

where superscripts 0 and 1 refer to the beginning and end of a time step:

$$\eta_j(x) = \frac{1}{\lambda_j^2 x}\left(1 - e^{-\lambda_j x}(1 + \lambda_j x)\right) \tag{3.11}$$

and:

$$\xi_j(x) = \frac{1}{\lambda_j^2 x}\left(\lambda_j x - 1 + e^{-\lambda_j x}\right) \tag{3.12}$$

The analytically integrated expressions for η_j and ξ_j allow arbitrary time steps. The η_j and ξ_j are numerically calculated only once during a time step and the computer time consumption is of no importance.

This methodology was successfully applied in [7] and [8]. A small FORTRAN code developed at VTT, which was provided to the benchmark team, utilises the above-described procedure and processes the data automatically. This code was used to alter participants' time histories for hot and cold leg coolant temperatures.

There are two thermo-couples and one thermo-resistor in each cold and hot leg of VVER-1000. The value of the temperature is the average of these three readings. The maximal values given by Gidropress for these constants are 30 s for thermo-couples and 2 s for thermo-resistor. The average time-delayed constant was used in our calculations.

Chapter 4

RESULTS AND DISCUSSION

4.1 Introduction

This chapter presents the comparative analyses of the results for Exercise 1 (point kinetics) of the Phase I of the VVER-1000 Coolant Transient Benchmark. The tables and figures in this chapter provide a comparison of the participants' results with the available plant data. The analyses of these results are grouped in two sections. In Section 4.2 the steady-state results at the initial conditions are discussed, and in Section 4.3 the analyses of the transient results are presented.

4.2 Steady-state results

Table 4.1 shows participants' models used for the simulation of Exercise 1. This table provides information not only about the general nodalisation but also information for the utilisation of the boundary conditions provided in the specification: steam generator (SG) feedwater, SG exit pressure, decay heat and MCP #3 rotor speed. This table, along with the answers to the questionnaire given in Appendix B, provides a good basis for the analyses of the participants' results

Table 4.1. Participants' models

	Name	SG FW BC	SG P BC	Decay heat	MCP #3 rotor speed BC	Vessel axial layers	Vessel t-h channels
1	**FZK**	NO	NO	YES	YES	20	14
2	**GRS**	YES	YES	YES	NO	24	1
3	**INRNE-1**	NO	NO	NO	YES	10	3
4	**INRNE-2**	NO	NO	NO	YES	22	6
5	**KI**	NO	NO	YES	NO	15	14
6	**KU**	NO	YES	NO	YES	10	48
7	**NRI**	NO	NO	YES	YES	14	11
8	**ORNL**	YES	YES	NO	YES	15	18
9	**PSU**	YES	YES	NO	YES	20	30
10	**UPISA**	YES	NO	NO	YES	48	28

This section contains the comparison of the steady-state results presented in Table 4.2 according to the requirements of the benchmark specification. The second column of the table presents the steady-state plant measured data, and the uncertainties of the measurement system are given in the third column. The remaining columns list the absolute deviations of the participants' results from the plant data.

The steady state results of all the participants converge within the specified uncertainty band with few exceptions. These exceptions and the results which significantly deviate from the plant data but are still within the uncertainty band are discussed below.

In general the steady-state results show better agreement for the cold leg coolant temperatures compared to the hot leg coolant temperatures due to the complex mixing in the upper plenum at the initial steady state. At the time before the transient begins the temperature of the coolant in hot leg #2 is lower than that in hot legs #1 and #4 because it is affected by the coolant with low temperature coming from loop #3 (the loop with the reversed flow). While the codes using the 3-D vessel model were generally able to predict this phenomenon, some of the codes that use single volumes to describe the upper plenum have difficulty predicting the exact situation. Thus, larger deviations are found in the results of such codes, and even UPISA's results for hot leg #1 are out of the uncertainty band.

In Table 4.2 one can see that flow rates of the loops and the core flow rate converge within the specified uncertainty band. However, the core flow rate for all of the participants deviates significantly from the plant data, while the deviations of the loops' flow rates are smaller. The reason is most probably that the plant data for the core flow rate does not take into account the core bypass flow; in other words, the plant data for the core flow rate represents approximately the sum of the flow rates in all four loops instead of the core flow rate itself. On the other hand, the reason for the scattered results for loop flow rates could be a result of the data for the homologous curves provided in the benchmark specification. Significant differences exist between the tabulated data and the plots for the homologous curves provided in the benchmark specification. Another possible reason could be the scatter of the plant data. The plant data indicates that the pressure drops for loops #1, #2 and #4 are 0.492 MPa, 0.469 MPa and 0.500 MPa, respectively, while the geometry of the loops provided in the specification is identical.

The converged steady state for all of the participants provides a good basis for the transient calculation.

4.3 Transient results

This section contains a summary of the comparisons of the transient results shown as plots and tables. The code-to-plant data comparisons are given for 129 seconds and the code-to-code comparisons are presented for 800 seconds. Overall, the participants' transient results are in good agreement, with a few exceptions discussed below.

Figure 4.1 shows the comparison of the participants' results for the pressuriser liquid level during the transient and Table 4.3 shows the FOM for each of the participants' results. The comparison of this parameter shows one of the largest deviations from the trend of the plant data among all of the compared parameters. At the beginning of the transient, the calculated value of the pressuriser level matches the measured value (Table 4.2). Later into the transient, the measured level decreases, whereas INRNE-2 and ORNL predict a slow increase in the trend. Most of the codes' predicted pressuriser levels stabilise earlier in the transient compared to the measured value, and at the end of the transient the pressuriser level is significantly higher. The reason for these significant differences is in the different models used by the participants as reported in the answers to the questionnaire in Appendix B. Some of the participants have make-up and let-down systems in their models, while others do not. Another source of these deviations is the different controller's logic of the make-up and let-down systems. Because of the initial lack of information in the benchmark specification some of the participants used simple logic for the controllers in order to more precisely predict the primary side pressure and the pressuriser level, while other participants utilised the real plant logic.

Initially, the comparison of the cold leg temperatures showed poor agreement between the calculated values and the plant data for some of the legs. The largest difference was observed in loop #3 in the interval from 7 to 14 seconds during the switching on of MCP #3 (Figure 4.5). All codes

Table 4.2. Steady-state results

Parameter	Plant data	Uncertainty	FZK	GRS	INRNE1	INRNE2	KI	KU	NRI	ORNL	PSU	UPISA
Core power, MW	824.000	±60.00	0.00	0.00	0.00	0.00	0.00	0.00	-0.01	26.00	0.00	0.00
Primary side pressure, MPa	15.60	±0.30	0.02	0.00	0.00	0.02	0.00	0.00	0.00	0.00	0.01	0.10
Cold leg #1 temperature, K	555.55	±2.00	-0.12	-1.30	-0.75	-0.26	-0.10	0.04	-0.81	0.00	-0.49	-0.77
Cold leg #2 temperature, K	554.55	±2.00	0.06	-1.16	-0.23	-0.36	-0.10	-0.28	-0.41	0.01	-0.35	0.22
Cold leg #3 temperature, K	554.35	±2.00	0.59	-0.42	0.22	0.34	0.40	0.15	-0.04	0.29	0.08	0.43
Cold leg #4 temperature, K	555.25	±2.00	-0.09	-1.16	-0.46	-0.10	-0.20	-0.02	-0.77	-0.04	-0.33	-0.48
Hot leg #1 temperature, K	567.05	±2.00	-0.87	-1.70	-1.89	-0.55	-0.30	-0.06	-1.53	0.41	-1.15	-2.30
Hot leg #2 temperature, K	562.85	±2.00	0.86	-1.25	0.88	-0.27	-0.20	-0.35	0.37	0.74	0.23	1.90
Hot leg #3 temperature, K	550.75	±2.00	-0.10	-0.77	-0.59	-0.18	-1.10	-0.59	-0.90	0.15	-0.68	0.18
Hot leg #4 temperature, K	566.15	±2.00	-0.72	-1.44	-0.99	-0.24	-0.90	-0.41	-1.69	0.06	-0.83	-1.40
Core flow rate, kg/s	13 611	±800	-34.00	51.50	-107.10	-49.00	20.00	-556.00	-225.90	NA	-146.60	64.00
Loop #1 flow rate, kg/s	5 031	±200	-10.00	-4.30	-22.82	-23.00	0.00	-30.40	-4.39	-117.44	-32.20	71.00
Loop #2 flow rate, kg/s	5 069	±200	-33.00	45.80	-41.93	-31.00	0.00	-53.30	-17.19	-119.61	-36.80	33.00
Loop #3 flow rate, kg/s	-1 544	±200	41.00	7.80	8.07	12.00	0.00	-6.60	-194.71	30.30	-41.00	-34.00
Loop #4 flow rate, kg/s	5 075	±200	-41.00	-18.00	-61.46	-27.00	0.00	-68.20	-29.59	-155.16	-56.60	27.00
Pressuriser level, m	7.44	±0.15	0.00	NA	0.00	-0.01	0.00	0.00	-0.01	0.00	0.00	0.00
Water level in SG1, m	2.30	±0.075	0.01	0.01	0.03	0.01	0.00	0.00	0.00	0.12	0.00	0.07
Water level in SG2, m	2.41	±0.075	0.00	0.00	0.00	0.00	0.00	0.00	-0.03	0.01	0.01	-0.04
Water level in SG3, m	2.49	±0.075	-0.05	0.00	-0.03	-0.02	0.02	0.00	0.01	-0.07	0.06	-0.04
Water level in SG4, m	2.43	±0.075	0.03	0.00	0.03	0.01	0.00	0.00	-0.04	-0.01	-0.01	-0.07
Secondary side pressure, MPa	5.94	±0.20	0.17	0.16	0.12	0.16	0.11	0.15	0.16	0.22	NA	0.20

predicted a sharp drop of the coolant temperature (approximately 4 to 5 K), though such a drop of the temperature could not be observed in the plant data. This phenomenon can be explained as follows. At the beginning, when the pump is off, the direction of the flow in this loop is reversed. After the pump starts, the flow that once has passed through the SG is forced back and goes trough the SG again, causing the temperature to decrease further. All codes predict the exact situation. However, the measurement did not register this temperature drop because of the time delay of the measurement system. In order to better compare the code predictions, a decision has been made that the benchmark team should incorporate the time delay of the measurement system into the participants' results. The time delay was incorporated (as explained in Chapter 3) and Figures 4.2 through 4.6 (excluding Figure 4.5) show the comparison of the updated participants' results to the plant measured data, while Tables 4.4 through 4.7 show the FOM for each of the participants' results. In each case, the participants' results are in reasonable agreement with the trend of the measured value. At the end of the transient all of the participants' results for all of the legs are within the uncertainty band of the measurement system.

As with the cold leg coolant temperatures, the comparison for hot legs initially showed poor agreement between the codes' predictions and the plant-measured values. The largest difference was observed in loop #2 in the interval from 0 to 20 s (Figure 4.9). The code predictions showed a peak of the temperature, while such a peak was not observed in the plant data. This temperature peak could be explained as follows. Before the transient starts the temperature of the coolant in hot leg #2 is lower than that in hot legs #1 and #4 because it is affected by the coolant with low temperature coming from loop #3 (the loop with the reversed flow). Only the temperature in loop #2 is affected because this loop is closest to loop #3. At the beginning of the transient, the flow in loop #3 reverses back and coolant with a higher temperature from loops #1 and #4 enters loop #2, which causes the peak of the temperature in the hot leg #2. Later into the transient, the coolant temperature in loops #1, #2 and #4 decreases due to the increasing flow through the core. Once again, the explanation for this significant difference is the time delay of the measurement system. The participants did not model the time delay of the thermo-couples in order not to introduce another source of error which could make the analyses of the results difficult. The time delay of the measurement system has been implemented into participants' results by the benchmark team, and Figures 4.7 through 4.11 (excluding Figure 4.9) show the comparison of the updated participants' results with plant-measured data. The incorporation of the time delay improved the comparison and allows a better analysis of the code predictions. In each case, the participants' results are in reasonable agreement with the trend of the measured value. The hot leg temperatures calculated by the benchmark participants fall within the range of the measurement uncertainty by the end of the transient.

Figure 4.12 provides a comparison of the pressure above the core. This comparison shows one of the largest deviations from the plant data among all of the compared parameters. This deviation, similar to the deviation for the pressuriser liquid level, is again a result of the different models used by the different participants as reported in the participants' answers to the questionnaire presented in Appendix B. Some of the participants model make-up and let-down systems while others do not. Similar differences in the models can also be observed for the pressuriser heaters. Make-up and let-down systems and the pressuriser heaters are of great importance for maintaining the primary pressure. The presence of these systems important, as is the type of the logic that has been applied in order to maintain them. The participants' answers to the questionnaire show that the logic used is also different, a point which was discussed earlier in this chapter.

The initial value of the reactor pressure drop (Table 4.14) predicted by the participants differs from the measured data for most of the participants. After the first 18 seconds into the transient, the calculated pressure drop converges to the measured value within the uncertainty range but the increase in the pressure drop is still different from the increase observed in the plant data (Figure 4.13). One

can observe similar behaviour for the MCP pressure drops in Figures 4.14 through 4.17 with few exceptions. Table 4.13 shows the FOM for each of the participants' results for reactor pressure drop. Tables 4.15 to 4.22 list the FOM and the initial values for the MCP #1 to #4 pressure drops. The differences observed in these results are due to the differences in the participants' models as reported in the answers to the questionnaire given in Appendix B. One variable is the different sets of pump characteristics used by the different participants. The deviations from the plant data are also enhanced by the reversed flow in loop #3 at the initial steady state.

The deviations in the heat-up trends for all four loops for all participants are within the specified uncertainty band (Figures 4.18 through 4.21). Tables 4.23 through 4.26 list the FOM for each of the participants' results. The use of a lower initial power level (824 MW_{th}) improved the results. Originally, the benchmark specification provided a higher value for the initial power. After some sensitivity studies on the power level performed at PSU, it was suggested that the lower power level provided by KNPP should be used. Later, the participants approved the suggested solution and agree to use the power level based on the secondary side parameters.

The reactor power and fission power levels predicted by all of the participants are shown in Figures 4.22 and 4.23. There are no available plant data for the reactor power during the transient. The reactor power predicted by all participants has the same initial value (except ORNL), and all the predictions show fairly good agreement at the end of the transient. However, the power trend predicted by PSU and INRNE-2 differs from those predicted by the rest of the participants. This difference is caused by the use of different heat-structure models. At PSU, the gas-gap conductance is a fixed value, while most of the participants use dynamical gas-gap conductance modelling. This difference in the gas-gap conductance model also reflects the observed differences in the total reactivity (Figure 4.24) and the fuel temperature (Figure 4.25). Another reason for these differences could be the model of the fuel rod. In TRAC-PF1 an annular fuel pellet is impossible to model explicitly.

Figure 4.26 shows a reasonably good agreement for the core average coolant temperature among the participants.

Figures 4.27 through 4.30 show the comparisons of the mass flow rates within each loop. Fairly good agreement exists between the different codes. The differences observed among the participants' results could be explained by the different pump characteristics used, as mentioned earlier.

Figure 4.1. Pressuriser water level change during the transient

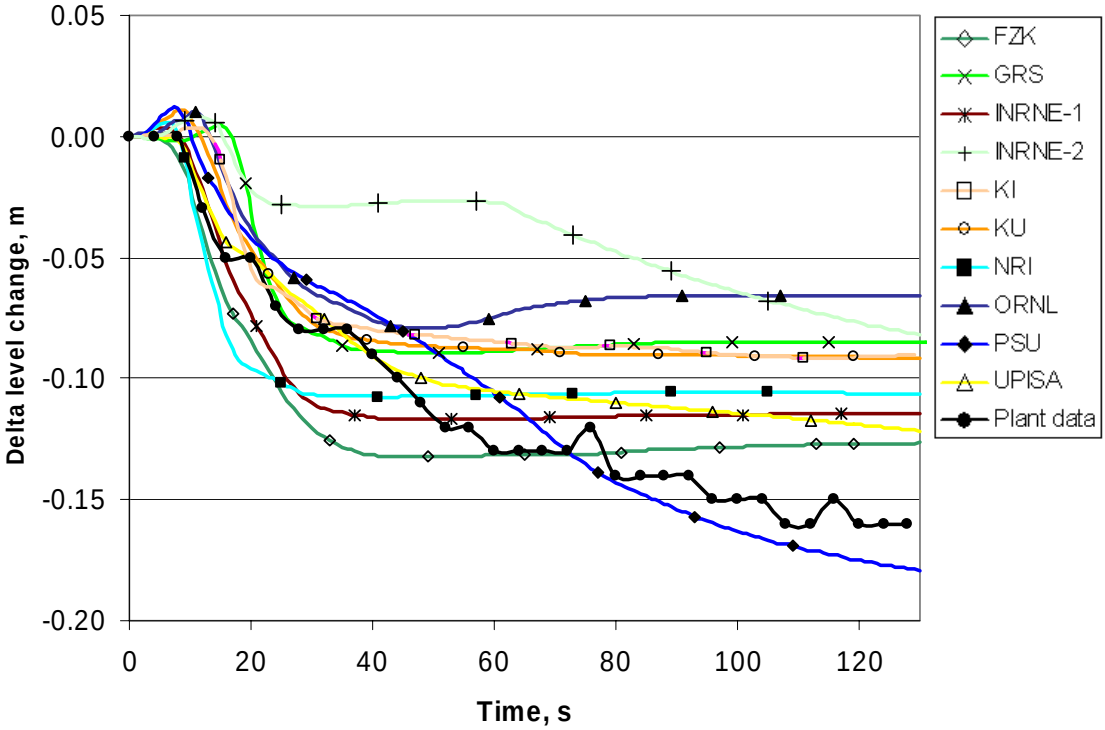

Table 4.3. Pressuriser water level FOM

	Participant	ME	VE	MSE	Combined
1	FZK	0.987416	0.978136	0.978144	0.981231
2	GRS	0.810862	0.972876	0.924150	0.902628
3	INRNE-1	0.937687	0.978052	0.974008	0.963248
4	INRNE-2	0.701761	0.972796	0.827564	0.834039
5	KI	0.814634	0.979334	0.932211	0.908725
6	KU	0.820920	0.979733	0.936228	0.912292
7	NRI	0.914649	0.968052	0.960192	0.947630
8	ORNL	0.760218	0.964731	0.880464	0.868470
9	PSU	0.980982	0.990723	0.990424	0.987375
10	UPISA	0.892457	0.991870	0.977847	0.954057

Figure 4.2. Cold leg #1 temperature change during the transient

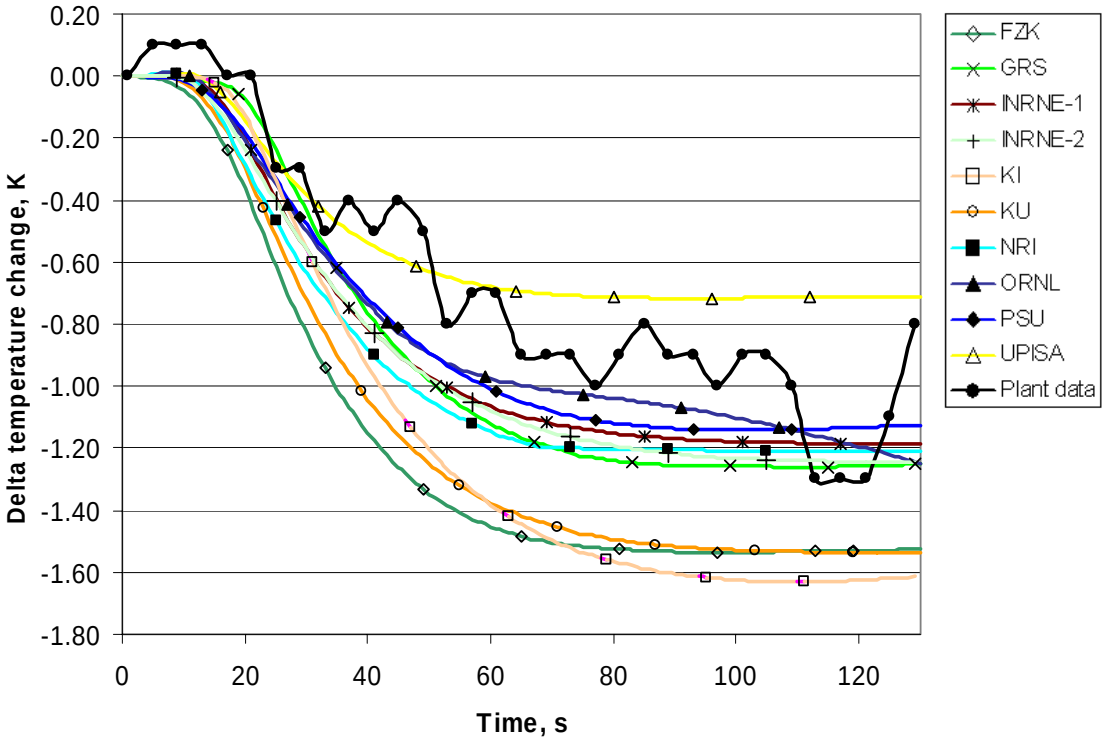

Table 4.4. Cold leg #1 coolant temperature FOM

	Participant	ME	VE	MSE	Combined
1	FZK	0.728348	0.977232	0.860417	0.855331
2	GRS	0.847835	0.987335	0.956992	0.930720
3	INRNE-1	0.859485	0.989600	0.964174	0.937752
4	INRNE-2	0.845202	0.990303	0.958533	0.931345
5	KI	0.744172	0.971015	0.871229	0.862138
6	KU	0.744971	0.979825	0.879023	0.867939
7	NRI	0.835526	0.987270	0.950981	0.924591
8	ORNL	0.887947	0.991827	0.976465	0.952079
9	PSU	0.883127	0.990812	0.973979	0.949305
10	UPISA	0.942648	0.979419	0.976034	0.966033

Figure 4.3. Cold leg #2 temperature change during the transient

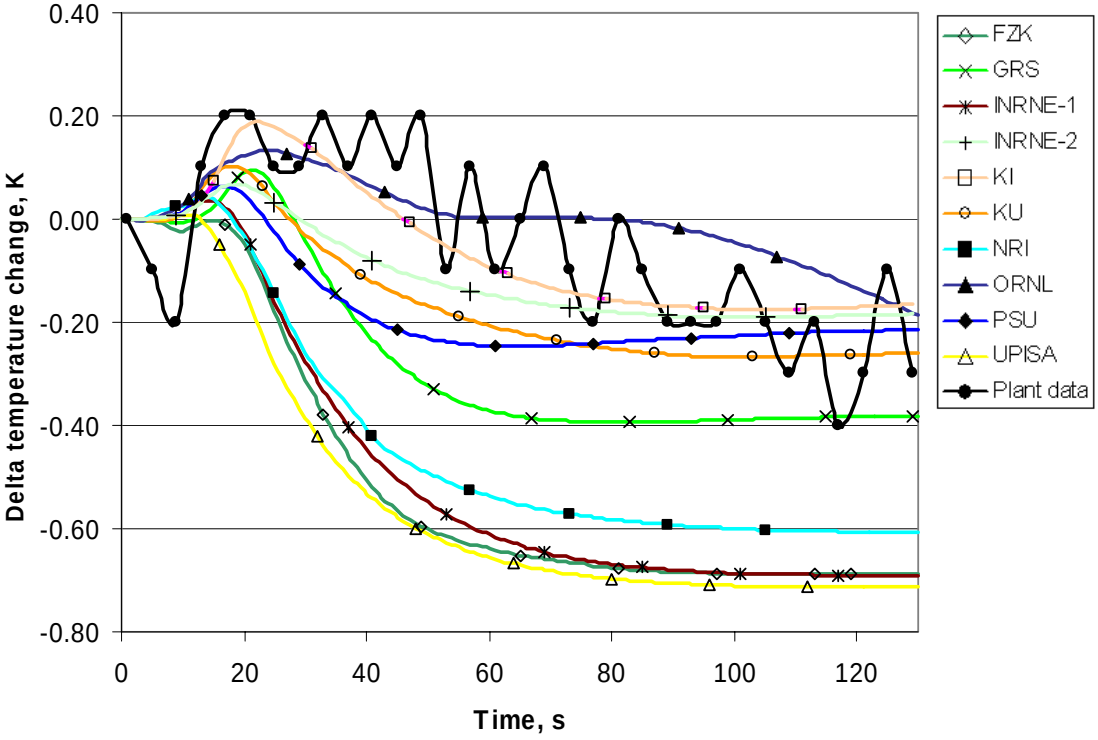

Table 4.5. Cold leg #2 coolant temperature FOM

	Participant	ME	VE	MSE	Combined
1	FZK	0.589444	0.879483	0.616858	0.695261
2	GRS	0.763571	0.937150	0.860269	0.853662
3	INRNE-1	0.600133	0.882842	0.634660	0.705878
4	INRNE-2	0.933727	0.958549	0.954243	0.948839
5	KI	0.991051	0.971568	0.971702	0.978106
6	KU	0.872123	0.958703	0.939631	0.923485
7	NRI	0.635626	0.900676	0.695385	0.743895
8	ORNL	0.903018	0.967962	0.957506	0.942828
9	PSU	0.862379	0.939709	0.918159	0.906748
10	UPISA	0.574905	0.875740	0.592576	0.681073

Figure 4.4. Cold leg #3 temperature change during the transient

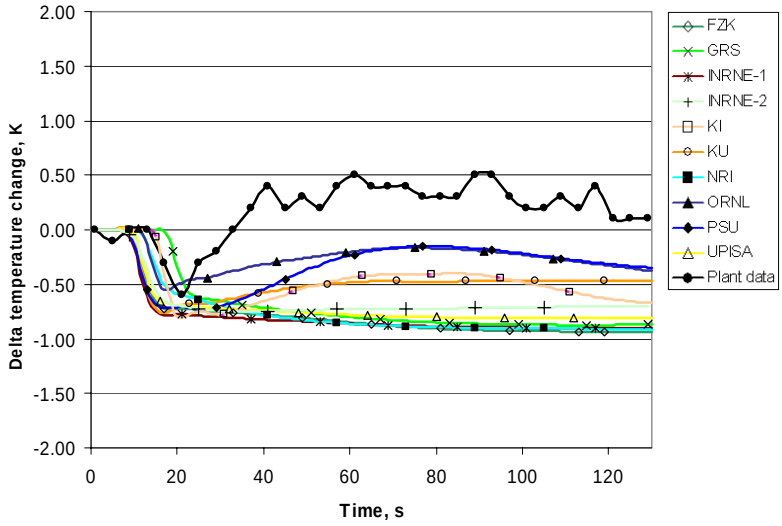

Figure 4.5. Cold leg #3 temperature during the transient (no time delay)

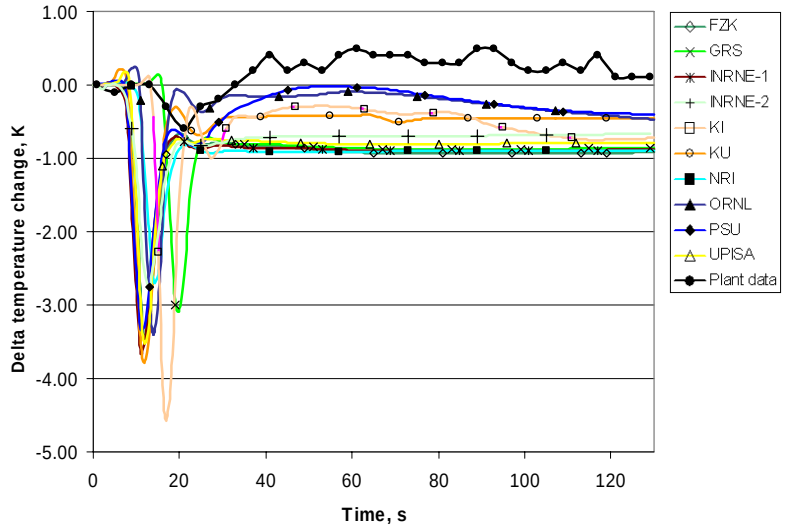

Table 4.6. Cold leg #3 coolant temperature FOM

	Participant	ME	VE	MSE	Combined
1	FZK	0.556265	0.874252	0.562092	0.664202
2	GRS	0.583462	0.841444	0.589393	0.671432
3	INRNE-1	0.554393	0.884668	0.563245	0.667434
4	INRNE-2	0.592919	0.902618	0.633535	0.709690
5	KI	0.648555	0.929365	0.730424	0.769447
6	KU	0.650369	0.941620	0.740451	0.777479
7	NRI	0.565761	0.855634	0.569302	0.663565
8	ORNL	0.744589	0.961217	0.863778	0.856527
9	PSU	0.710308	0.965354	0.831982	0.835880
10	UPISA	0.577882	0.889103	0.603374	0.690119

Figure 4.6. Cold leg #4 temperature change during the transient

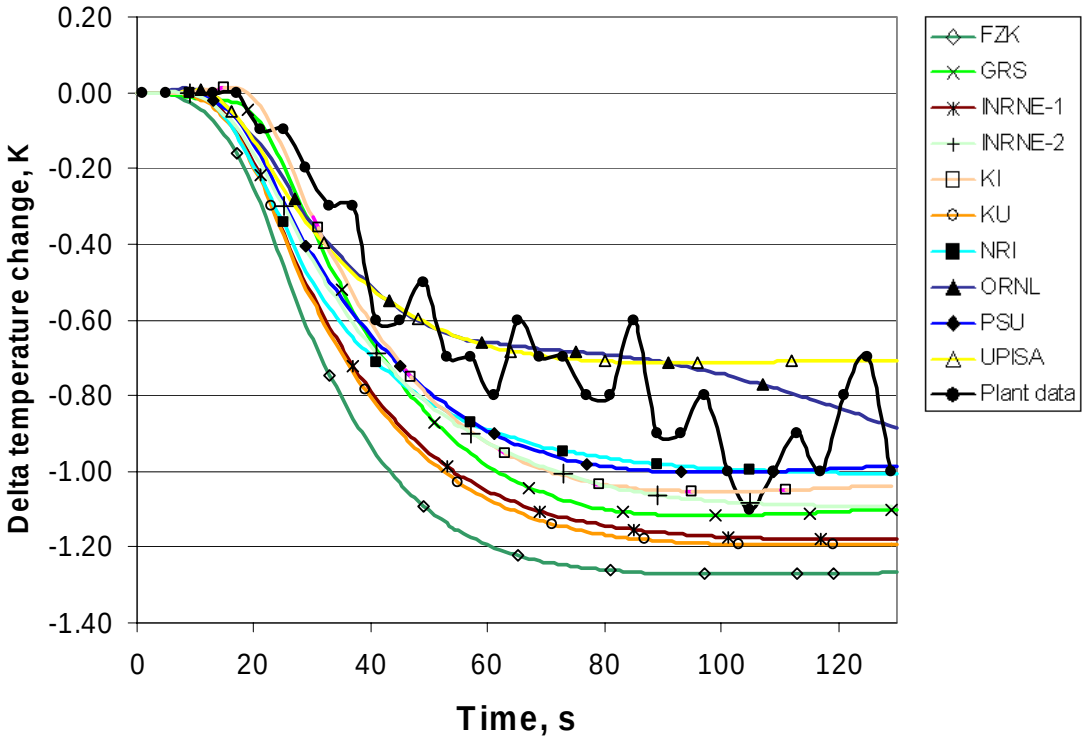

Table 4.7. Cold leg #4 coolant temperature FOM

	Participant	ME	VE	MSE	Combined
1	FZK	0.750910	0.975879	0.881395	0.869394
2	GRS	0.852363	0.984932	0.956770	0.931354
3	INRNE-1	0.806695	0.983351	0.930907	0.906983
4	INRNE-2	0.860679	0.989178	0.964265	0.938039
5	KI	0.887250	0.987060	0.971668	0.948658
6	KU	0.797147	0.982432	0.923785	0.901120
7	NRI	0.884219	0.988918	0.972511	0.948548
8	ORNL	0.969470	0.988234	0.987355	0.981685
9	PSU	0.892695	0.989623	0.975748	0.952688
10	UPISA	0.953833	0.983966	0.981822	0.973206

Figure 4.7. Hot leg #1 temperature change during the transient

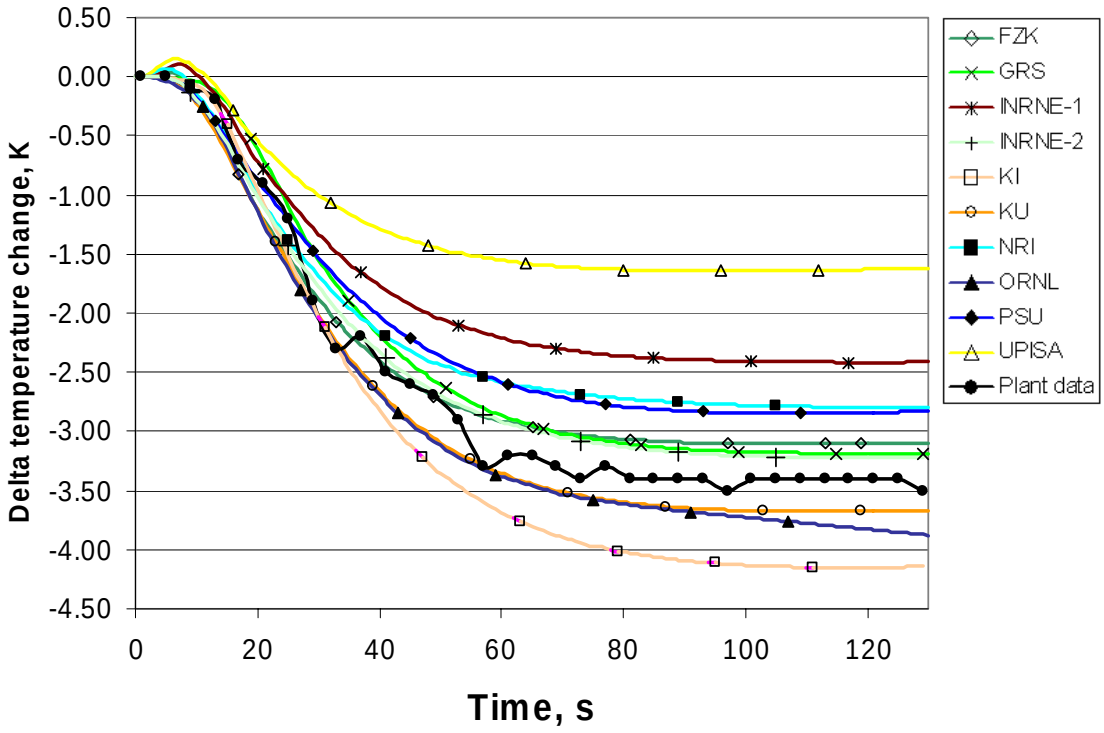

Table 4.8. Hot leg #1 coolant temperature FOM

	Participant	ME	VE	MSE	Combined
1	FZK	0.957656	0.996757	0.994843	0.983084
2	GRS	0.939091	0.998940	0.994768	0.977599
3	INRNE-1	0.826299	0.989798	0.948390	0.921495
4	INRNE-2	0.963972	0.998112	0.996737	0.986273
5	KI	0.882232	0.993676	0.976434	0.950780
6	KU	0.942284	0.999059	0.995335	0.978892
7	NRI	0.895648	0.993334	0.980167	0.956382
8	ORNL	0.931183	0.998626	0.993219	0.974341
9	PSU	0.894928	0.994916	0.981494	0.957112
10	UPISA	0.732006	0.970751	0.859154	0.853969

Figure 4.8. Hot leg #2 temperature change during the transient

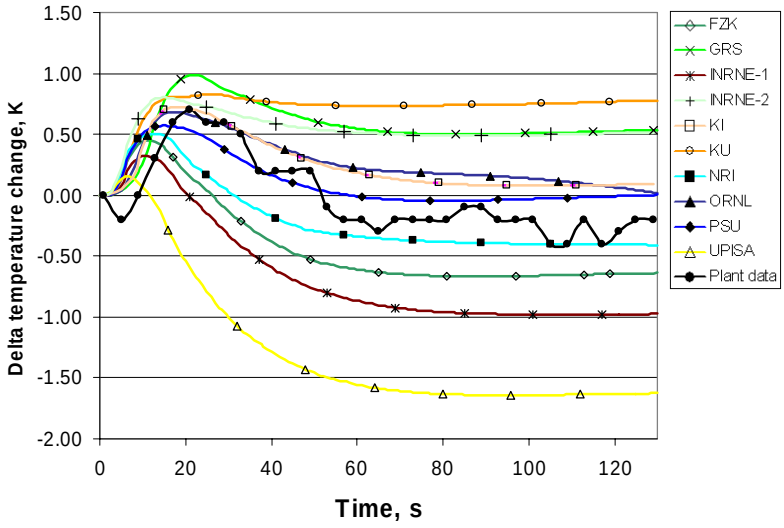

Figure 4.9. Hot leg #2 temperature change during the transient (no time delay)

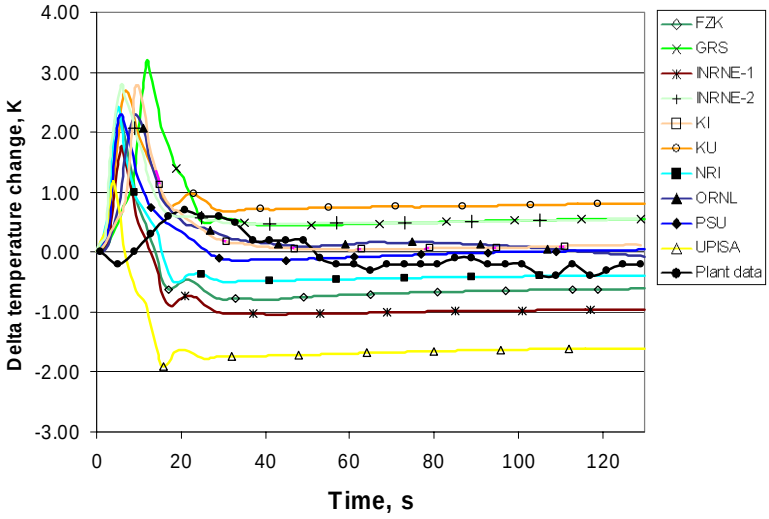

Table 4.9. Hot leg #2 coolant temperature FOM

	Participant	ME	VE	MSE	Combined
1	FZK	0.783827	0.949714	0.886049	0.873196
2	GRS	0.637153	0.960137	0.732327	0.776538
3	INRNE-1	0.670900	0.930151	0.760372	0.787140
4	INRNE-2	0.646397	0.953145	0.741821	0.780453
5	KI	0.776302	0.986072	0.911534	0.891302
6	KU	0.587475	0.923248	0.634686	0.715136
7	NRI	0.916709	0.962270	0.954959	0.944645
8	ORNL	0.766003	0.981602	0.899348	0.882317
9	PSU	0.853242	0.976137	0.948907	0.926094
10	UPISA	0.496497	0.847663	0.453152	0.599103

Figure 4.10. Hot leg #3 temperature change during the transient

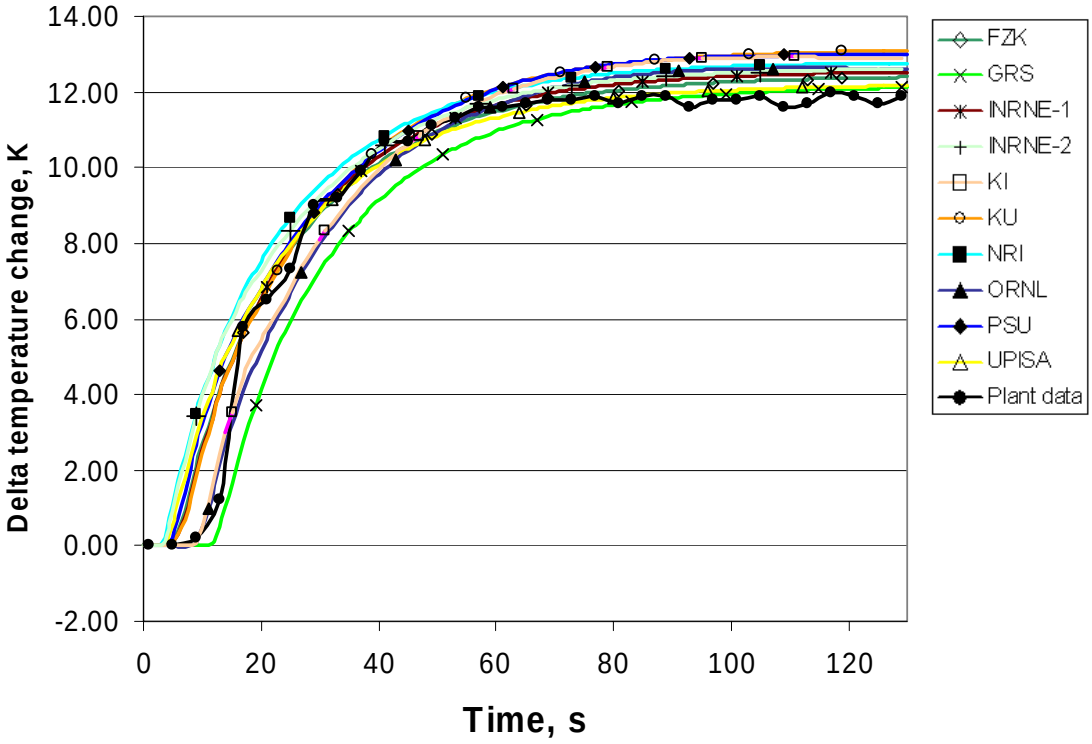

Table 4.10. Hot leg #3 coolant temperature FOM

	Participant	ME	VE	MSE	Combined
1	FZK	0.973454	0.997382	0.996663	0.989165
2	GRS	0.960714	0.995702	0.994079	0.983498
3	INRNE-1	0.964704	0.997729	0.996415	0.986282
4	INRNE-2	0.943474	0.995420	0.991911	0.976934
5	KI	0.967520	0.996331	0.995242	0.986364
6	KU	0.939343	0.997419	0.993307	0.976689
7	NRI	0.929915	0.995780	0.990211	0.971968
8	ORNL	0.985553	0.996766	0.996577	0.992964
9	PSU	0.935114	0.996705	0.991970	0.974595
10	UPISA	0.977462	0.995821	0.995326	0.989536

Figure 4.11. Hot leg #4 temperature change during the transient

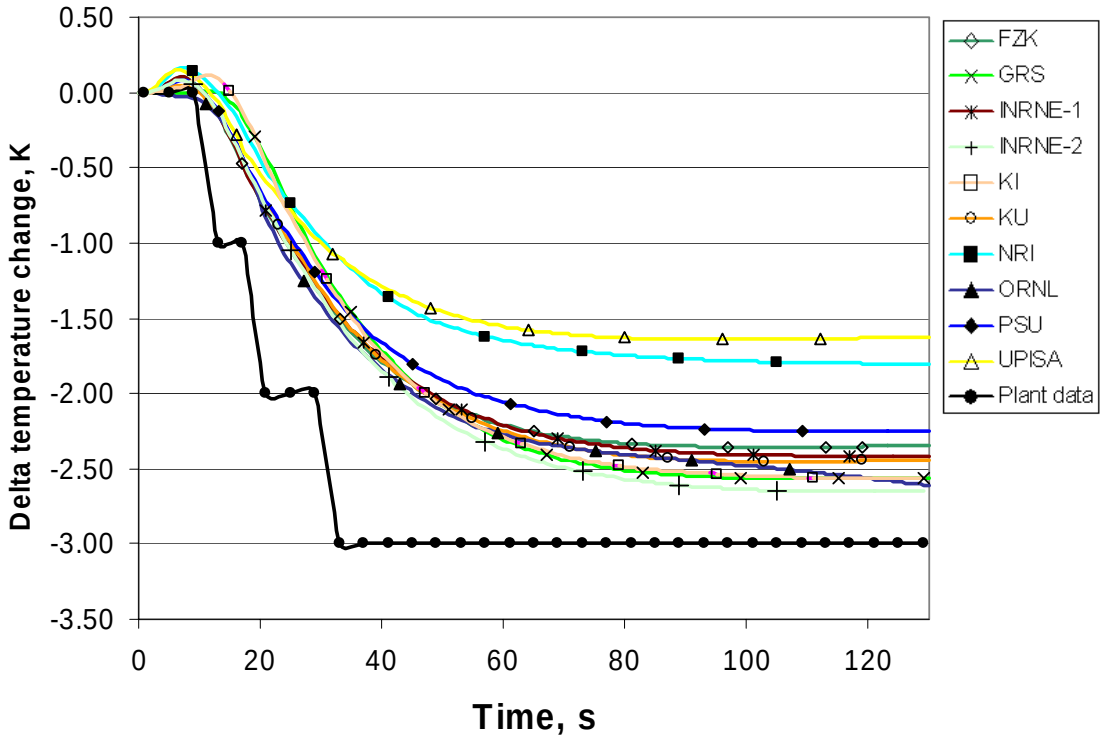

Table 4.11. Hot leg #4 coolant temperature FOM

	Participant	ME	VE	MSE	Combined
1	FZK	0.808887	0.991138	0.939237	0.913086
2	GRS	0.821300	0.984257	0.940544	0.915366
3	INRNE-1	0.812761	0.990424	0.941028	0.914737
4	INRNE-2	0.842732	0.988716	0.955884	0.929110
5	KI	0.819594	0.985414	0.940609	0.915205
6	KU	0.817744	0.989655	0.943354	0.916917
7	NRI	0.725183	0.985077	0.863076	0.857778
8	ORNL	0.828397	0.990141	0.949855	0.922797
9	PSU	0.788436	0.989530	0.923786	0.900583
10	UPISA	0.712991	0.982774	0.847864	0.847876

Figure 4.12. Pressure above the core change during the transient

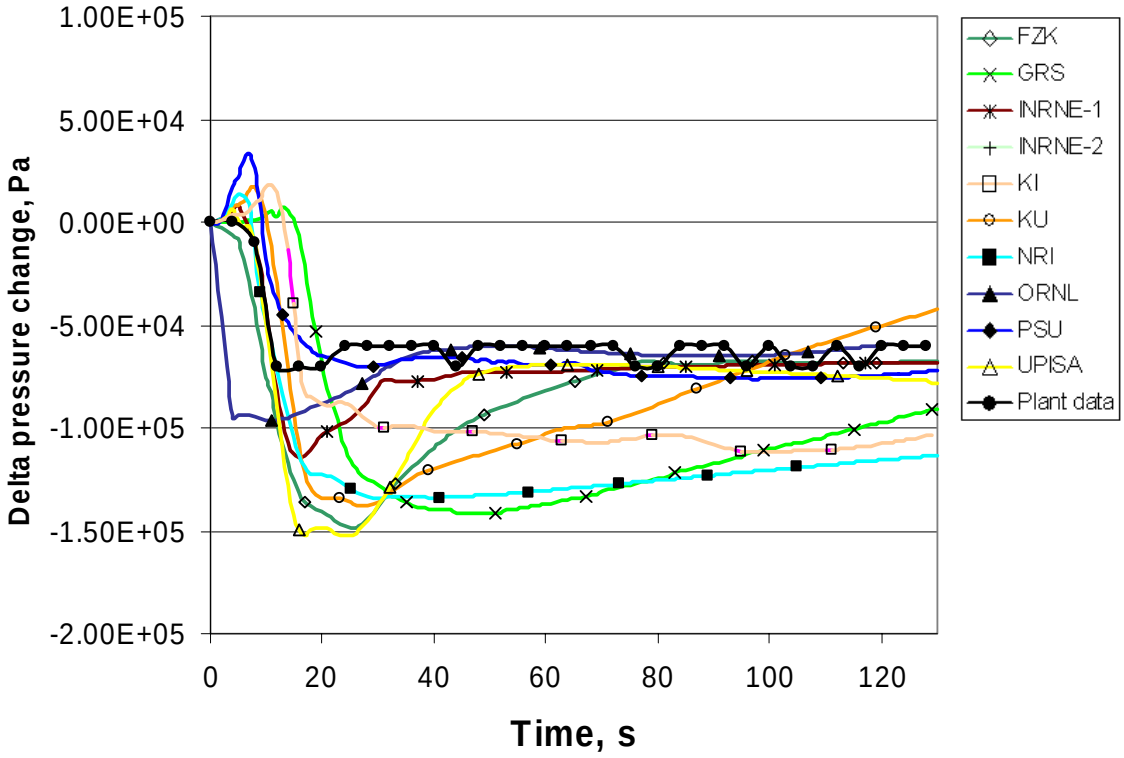

Table 4.12. Pressure above the core FOM

	Participant	ME	VE	MSE	Combined
1	FZK	0.759143	0.894402	0.821135	0.824893
2	GRS	0.636618	0.801540	0.636326	0.691494
3	INRNE-1	0.873932	0.979633	0.960208	0.937923
4	KI	0.703941	0.891197	0.770394	0.788510
5	KU	0.764982	0.850888	0.788463	0.801443
6	NRI	0.582672	0.924809	0.627482	0.711654
7	ORNL	0.896353	0.927839	0.916968	0.913719
8	PSU	0.940374	0.976218	0.972577	0.963055
9	UPISA	0.778097	0.889869	0.830463	0.832809

Figure 4.13. Reactor pressure drop change during the transient

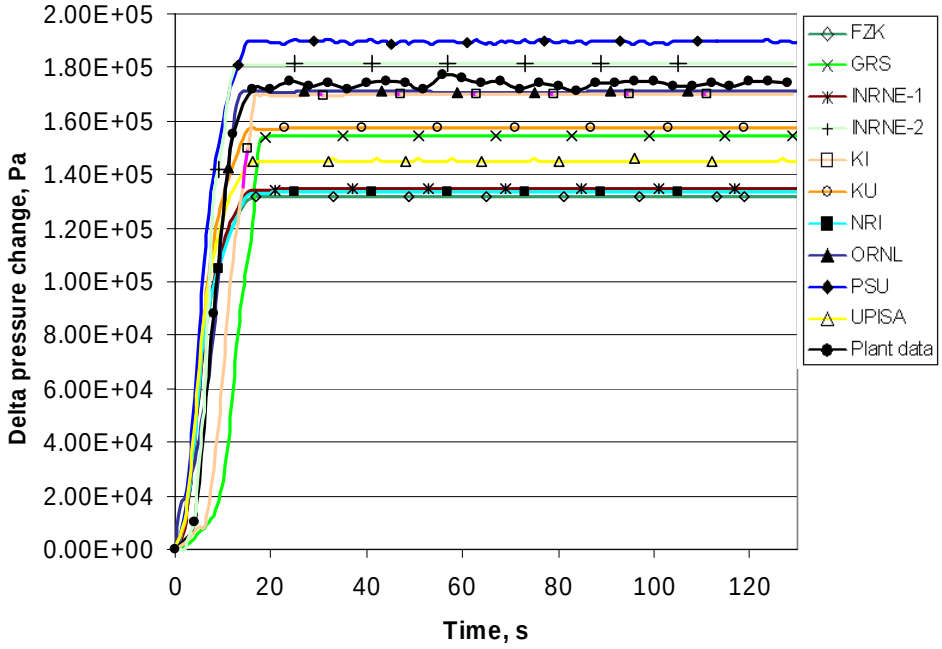

Table 4.13. Reactor pressure drop FOM

	Participant	ME	VE	MSE	Combined
1	FZK	0.828897	0.992051	0.951872	0.924272
2	GRS	0.884221	0.990726	0.974246	0.949730
3	INRNE-1	0.839116	0.992673	0.957776	0.929854
4	INRNE-2	0.954558	0.999023	0.996773	0.983450
5	KI	0.961557	0.995563	0.994015	0.983711
6	KU	0.931969	0.995920	0.990694	0.972860
7	NRI	0.834223	0.992019	0.954678	0.926972
8	ORNL	0.990701	0.999292	0.999209	0.996400
9	PSU	0.909824	0.997695	0.988029	0.965182
10	UPISA	0.880301	0.993398	0.975529	0.949742

Table 4.14. Reactor pressure drop initial values

Participant	Result, Pa
Plant data	2.25E+05 +/-0.40E+05
FZK	2.58E+05
GRS	2.58E+05
INRNE-1	2.65E+05
INRNE-2	2.01E+05
KI	2.29E+05
KU	2.24E+05
NRI	2.66E+05
ORNL	2.30E+05
PSU	1.86E+05
UPISA	2.13E+05

Figure 4.14. MCP #1 pressure drop change during the transient

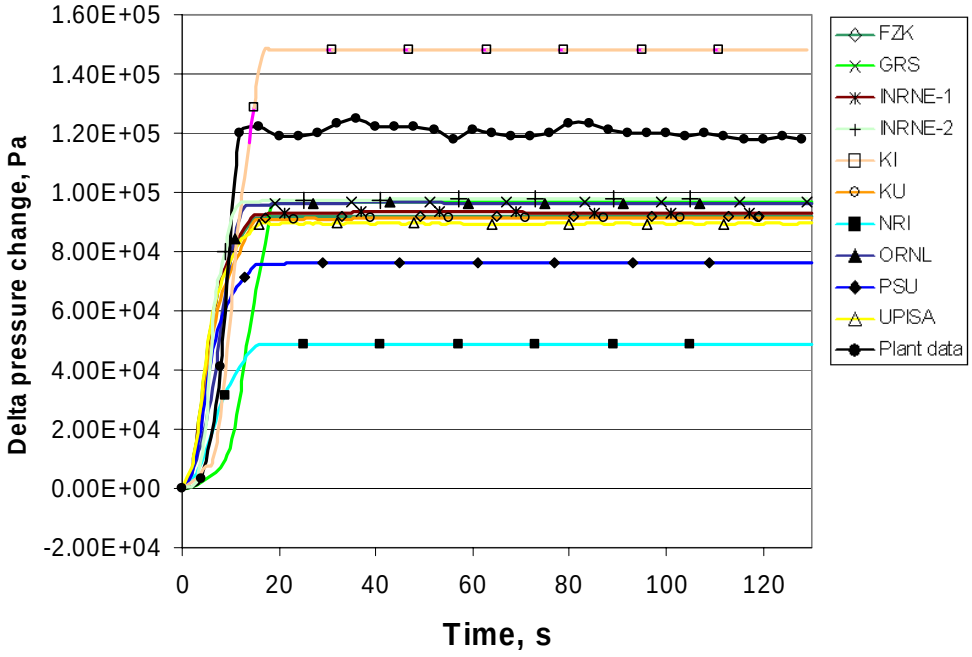

Table 4.15. MCP #1 pressure drop FOM

	Participant	ME	VE	MSE	Combined
1	FZK	0.839504	0.988569	0.954176	0.927416
2	GRS	0.834484	0.989333	0.952345	0.925386
3	INRNE-1	0.845317	0.989097	0.957466	0.930626
4	INRNE-2	0.867203	0.992483	0.969965	0.943216
5	KI	0.847113	0.989361	0.958548	0.931673
6	KU	0.832358	0.990076	0.951917	0.924783
7	NRI	0.659892	0.978718	0.776871	0.805159
8	ORNL	0.857118	0.994876	0.968148	0.940046
9	PSU	0.763805	0.985207	0.900474	0.883161
10	UPISA	0.826874	0.987300	0.946429	0.920200

Table 4.16. MCP #1 pressure drop initial value

Participant	Result, Pa
Plant data	4.92E+05 +/-0.40E+05
FZK	4.84E+05
GRS	5.22E+05
INRNE-1	4.90E+05
INRNE-2	5.14E+05
KI	4.41E+05
KU	5.15E+05
NRI	6.41E+05
ORNL	5.06E+05
PSU	5.46E+05
UPISA	4.99E+05

Figure 4.15. MCP #2 pressure drop change during the transient

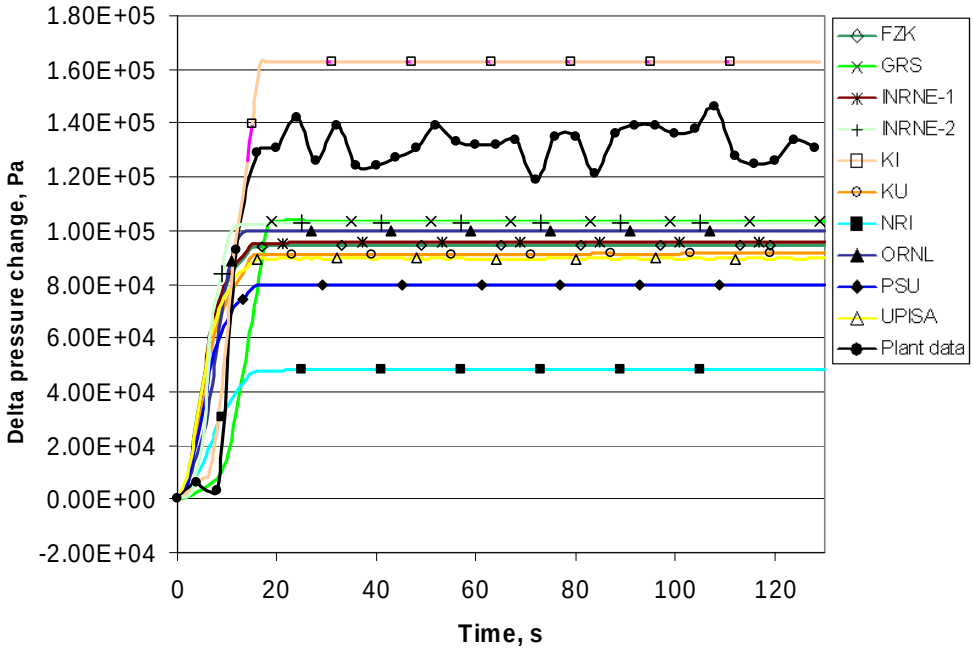

Table 4.17. MCP #2 pressure drop FOM

	Participant	ME	VE	MSE	Combined
1	FZK	0.830037	0.978478	0.940065	0.916192
2	GRS	0.843401	0.993940	0.961052	0.932797
3	INRNE-1	0.833960	0.978933	0.942511	0.918467
4	INRNE-2	0.865380	0.981989	0.959324	0.935563
5	KI	0.843723	0.995632	0.962778	0.934043
6	KU	0.813892	0.979749	0.932141	0.908593
7	NRI	0.665119	0.969699	0.778506	0.804440
8	ORNL	0.849797	0.985529	0.956194	0.930506
9	PSU	0.769229	0.976219	0.897524	0.880990
10	UPISA	0.808811	0.976677	0.926291	0.903926

Table 4.18. MCP #2 pressure drop initial value

Participant	Result, Pa
Plant data	4.69E+05 +/-0.40E+05
FZK	4.82E+05
GRS	5.10E+05
INRNE-1	4.88E+05
INRNE-2	5.11E+05
KI	4.26E+05
KU	5.15E+05
NRI	6.40E+05
ORNL	5.01E+05
PSU	5.42E+05
UPISA	4.99E+05

Figure 4.16. MCP #3 pressure drop change during the transient

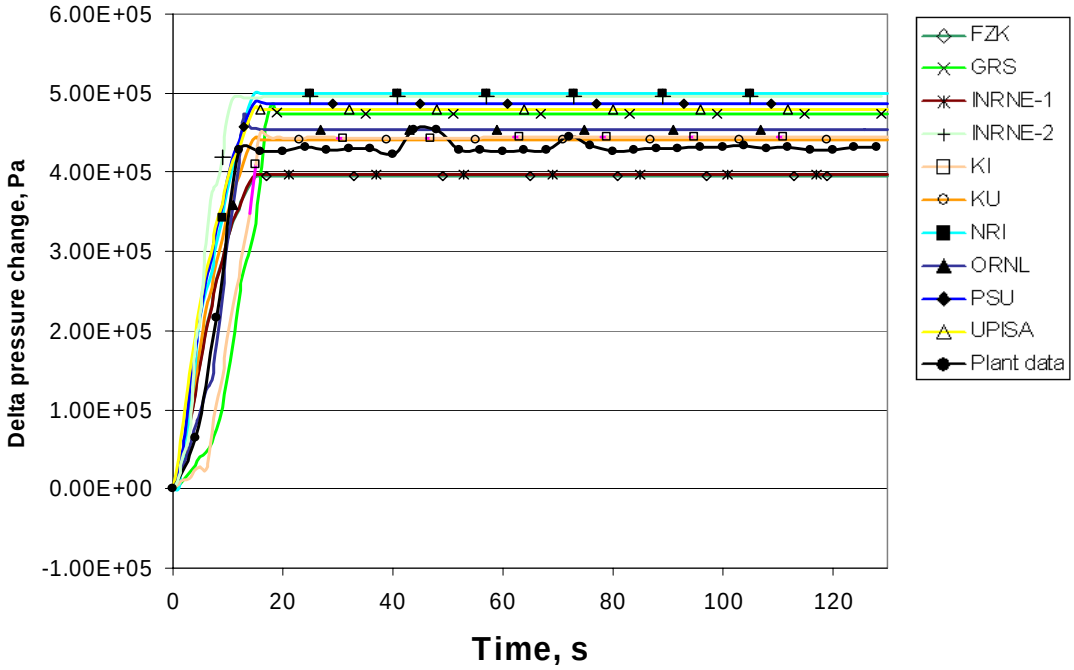

Table 4.19. MCP #3 pressure drop FOM

	Participant	ME	VE	MSE	Combined
1	FZK	0.937731	0.997510	0.993160	0.976133
2	GRS	0.948739	0.986098	0.983371	0.972735
3	INRNE-1	0.939238	0.997643	0.993513	0.976797
4	INRNE-2	0.872147	0.997019	0.976127	0.948430
5	KI	0.997773	0.993424	0.993468	0.994887
6	KU	0.975272	0.998498	0.997869	0.990545
7	NRI	0.873137	0.998530	0.977927	0.949864
8	ORNL	0.960702	0.999213	0.997551	0.985821
9	PSU	0.891058	0.998489	0.983817	0.957787
10	UPISA	0.900491	0.997982	0.985981	0.961483

Table 4.20. MCP #3 pressure drop initial value

Participant	Result, Pa
Plant data	1.79E+05 +/-0.40E+05
FZK	1.81E+05
GRS	1.35E+05
INRNE-1	1.87E+05
INRNE-2	1.21E+05
KI	1.50E+05
KU	1.66E+05
NRI	1.42E+05
ORNL	1.50E+05
PSU	1.36E+05
UPISA	1.09E+05

Figure 4.17. MCP #4 pressure drop change during the transient

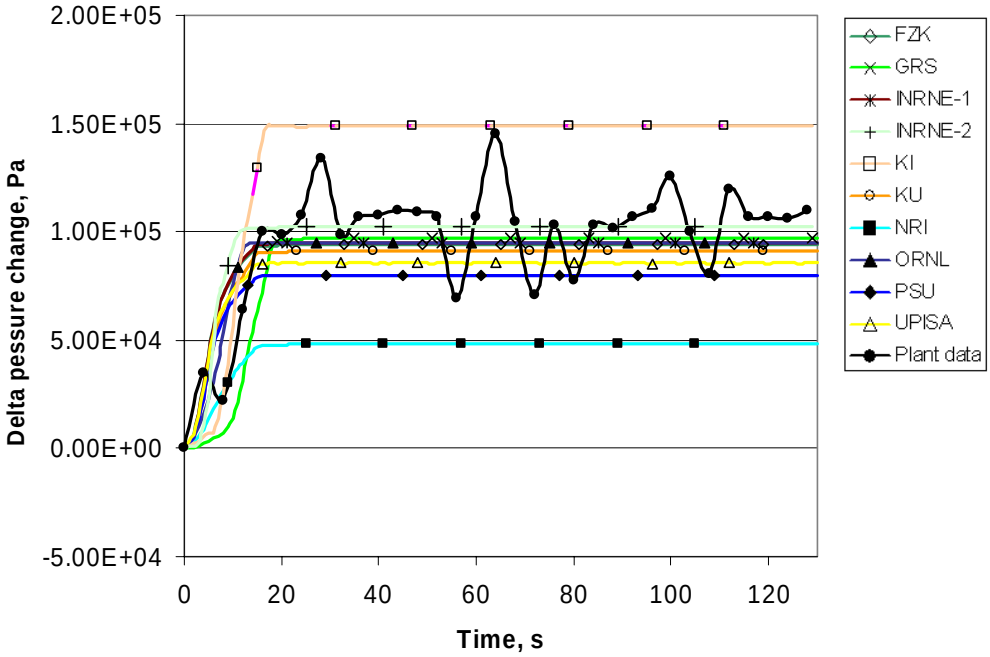

Table 4.21. MCP #4 pressure drop FOM

	Participant	ME	VE	MSE	Combined
1	FZK	0.949613	0.984366	0.981763	0.971913
2	GRS	0.934525	0.988642	0.983952	0.969038
3	INRNE-1	0.954920	0.984481	0.982442	0.973946
4	INRNE-2	0.999085	0.983589	0.983712	0.988794
5	KI	0.789206	0.979013	0.915237	0.894485
6	KU	0.929838	0.985352	0.979963	0.965050
7	NRI	0.736227	0.981340	0.871663	0.863076
8	ORNL	0.949620	0.986489	0.983859	0.973322
9	PSU	0.872667	0.983373	0.963326	0.939788
10	UPISA	0.903383	0.983743	0.972916	0.953347

Table 4.22. MCP #4 pressure drop initial value

Participant	Result, Pa
Plant data	5.00E+05 +/-0.40E+05
FZK	4.82E+05
GRS	5.17E+05
INRNE-1	4.89E+05
INRNE-2	5.06E+05
KI	4.44E+05
KU	5.15E+05
NRI	6.40E+05
ORNL	5.06E+05
PSU	5.42E+05
UPISA	5.17E+05

Figure 4.18. Heat-up in loop #1 change during the transient

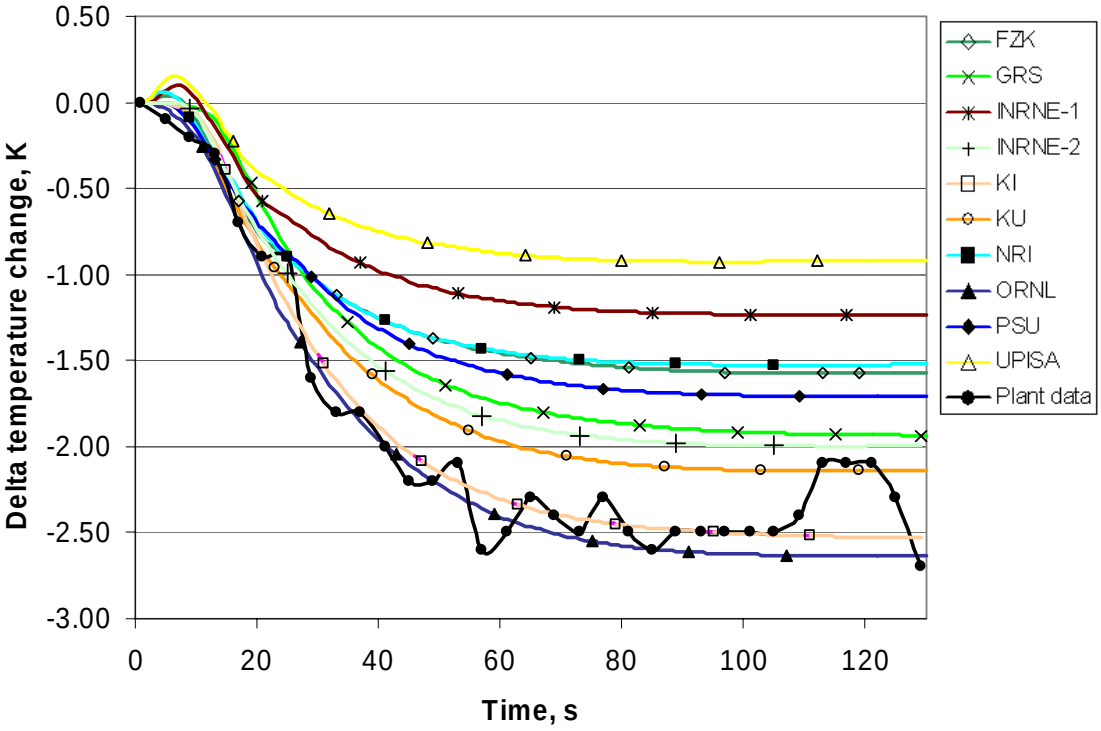

Table 4.23. Heat-up in loop #1 FOM

	Participant	ME	VE	MSE	Combined
1	FZK	0.802812	0.985255	0.930076	0.906047
2	GRS	0.853487	0.994018	0.965773	0.937758
3	INRNE-1	0.744578	0.978799	0.877829	0.867068
4	INRNE-2	0.878077	0.994203	0.975547	0.949275
5	KI	0.992907	0.996029	0.996008	0.994980
6	KU	0.908580	0.995006	0.985120	0.962901
7	NRI	0.797987	0.984740	0.926385	0.903037
8	ORNL	0.972277	0.995745	0.994972	0.987664
9	PSU	0.823742	0.988598	0.945869	0.919402
10	UPISA	0.700605	0.969857	0.824090	0.831517

Figure 4.19. Heat-up in loop #2 change during the transient

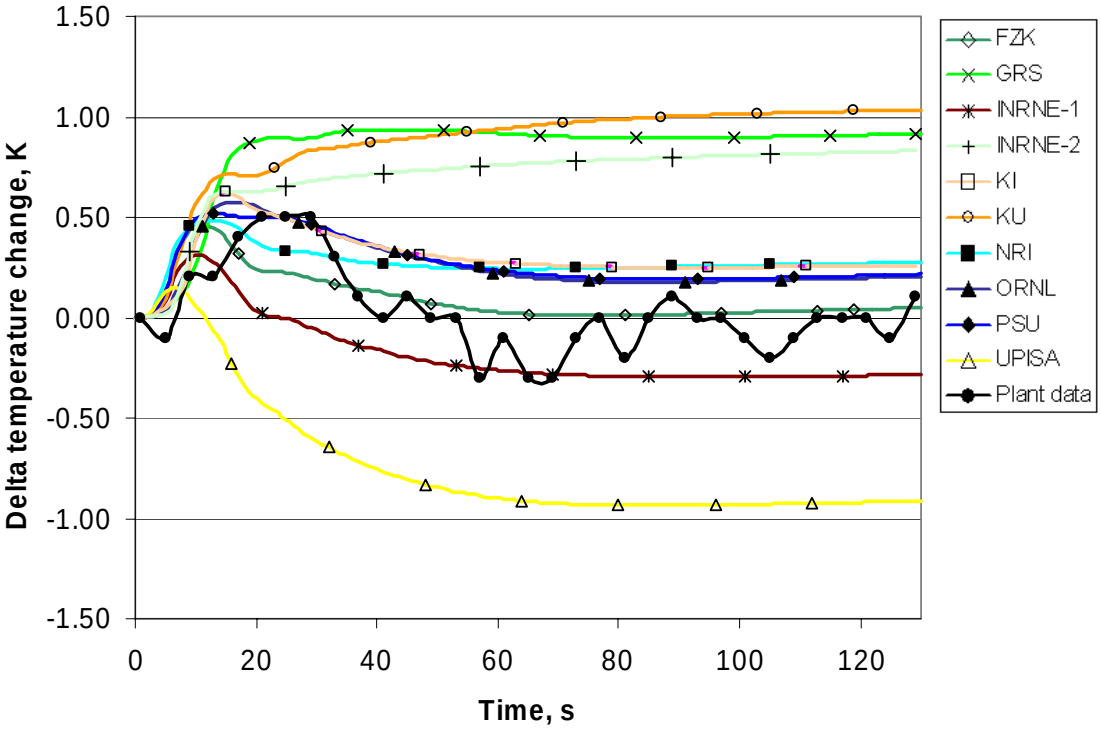

Table 4.24. Heat-up in loop #2 FOM

	Participant	ME	VE	MSE	Combined
1	FZK	0.878187	0.967088	0.949656	0.931643
2	GRS	0.503382	0.873184	0.472270	0.616278
3	INRNE-1	0.850133	0.960087	0.932547	0.914255
4	INRNE-2	0.542706	0.881525	0.542482	0.655570
5	KI	0.725351	0.968092	0.850283	0.847908
6	KU	0.490509	0.853681	0.444645	0.596278
7	NRI	0.741643	0.956941	0.857628	0.852070
8	ORNL	0.751707	0.974920	0.881344	0.869322
9	PSU	0.743035	0.974037	0.872562	0.863211
10	UPISA	0.550099	0.893664	0.559607	0.667789

Figure 4.20. Heat-up in loop #3 change during the transient

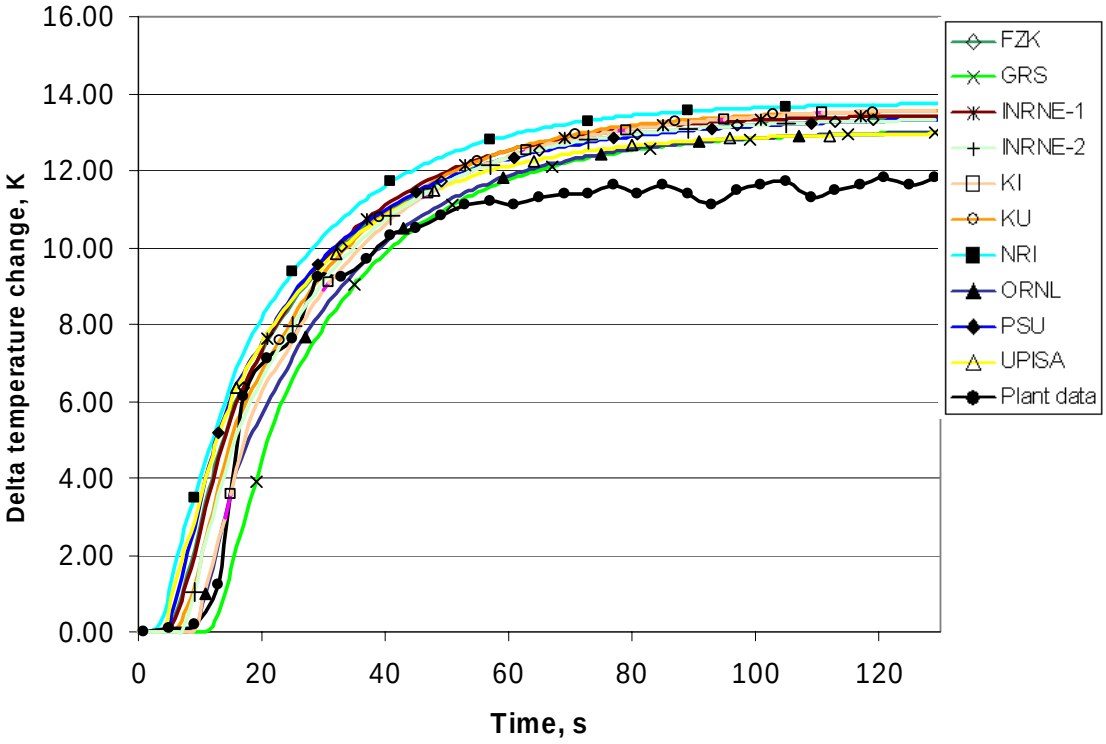

Table 4.25. Heat-up in loop #3 FOM

	Participant	ME	VE	MSE	Combined
1	FZK	0.905636	0.997011	0.986357	0.963000
2	GRS	0.973267	0.991103	0.990430	0.984933
3	INRNE-1	0.898337	0.997088	0.984538	0.959986
4	INRNE-2	0.918743	0.996388	0.988709	0.967946
5	KI	0.920976	0.994472	0.987285	0.967577
6	KU	0.904482	0.996142	0.985226	0.961949
7	NRI	0.866867	0.996735	0.973864	0.945821
8	ORNL	0.954523	0.995466	0.993256	0.981081
9	PSU	0.901522	0.996652	0.984964	0.961045
10	UPISA	0.914753	0.996831	0.988299	0.966627

Figure 4.21. Heat-up in loop #4 change during the transient

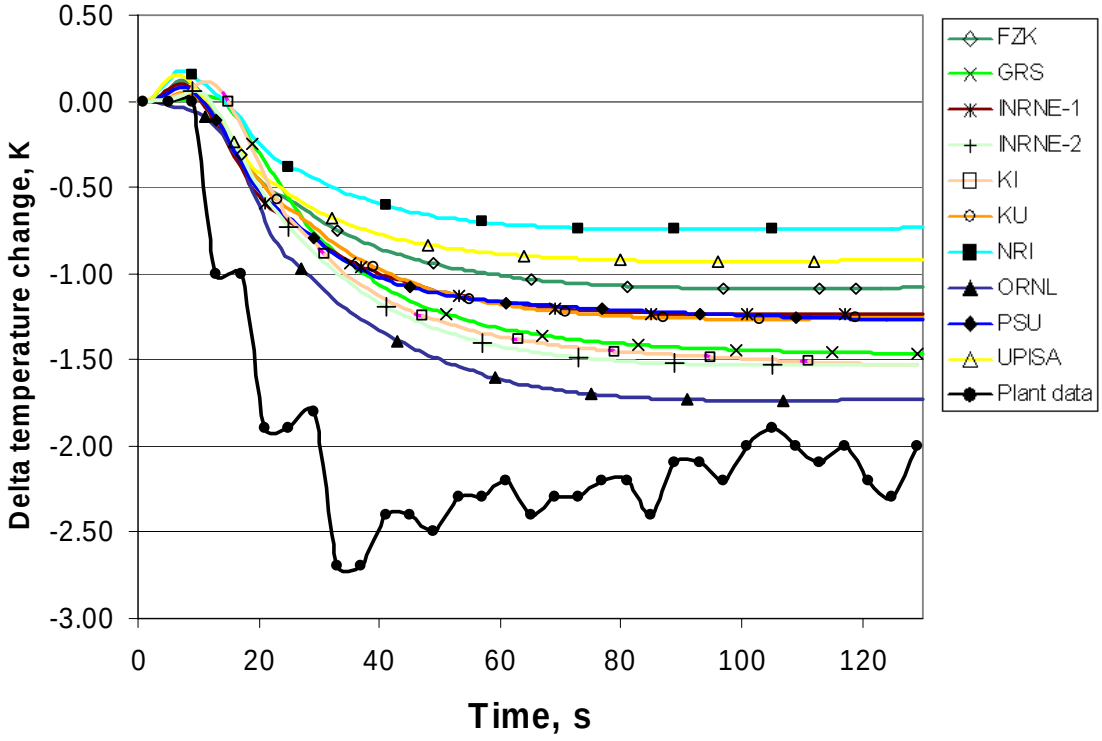

Table 4.26. Heat-up in loop #4 FOM

	Participant	ME	VE	MSE	Combined
1	FZK	0.721928	0.979759	0.855531	0.852405
2	GRS	0.766453	0.979990	0.898383	0.881608
3	INRNE-1	0.746062	0.982504	0.882205	0.870256
4	INRNE-2	0.785371	0.982926	0.915817	0.894704
5	KI	0.775627	0.981700	0.907292	0.888205
6	KU	0.746000	0.981144	0.881057	0.869399
7	NRI	0.676558	0.974479	0.797105	0.816046
8	ORNL	0.823066	0.983790	0.941120	0.915991
9	PSU	0.746602	0.982580	0.882779	0.870653
10	UPISA	0.702989	0.978316	0.832986	0.838096

Figure 4.22. Reactor power change during the transient

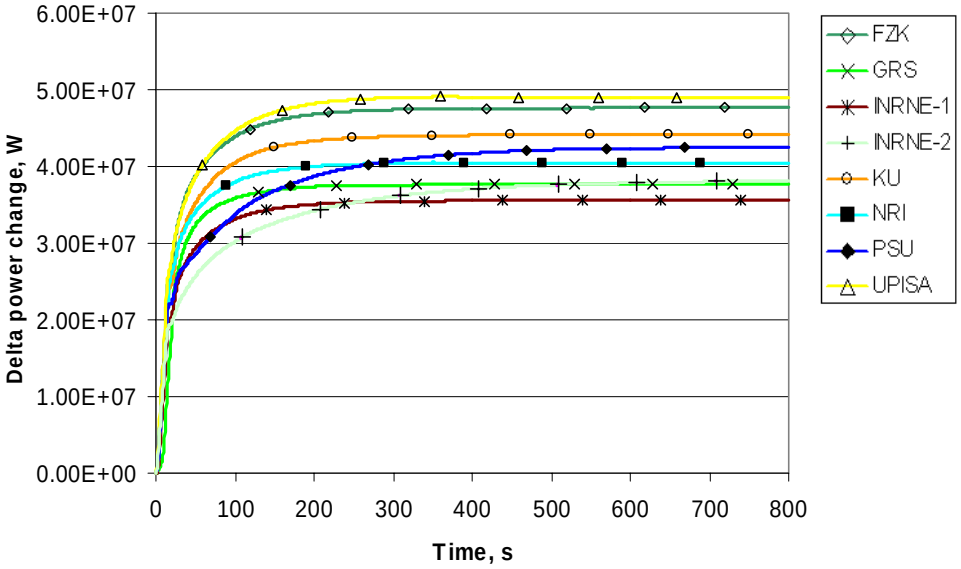

Figure 4.23. Fission power change during the transient

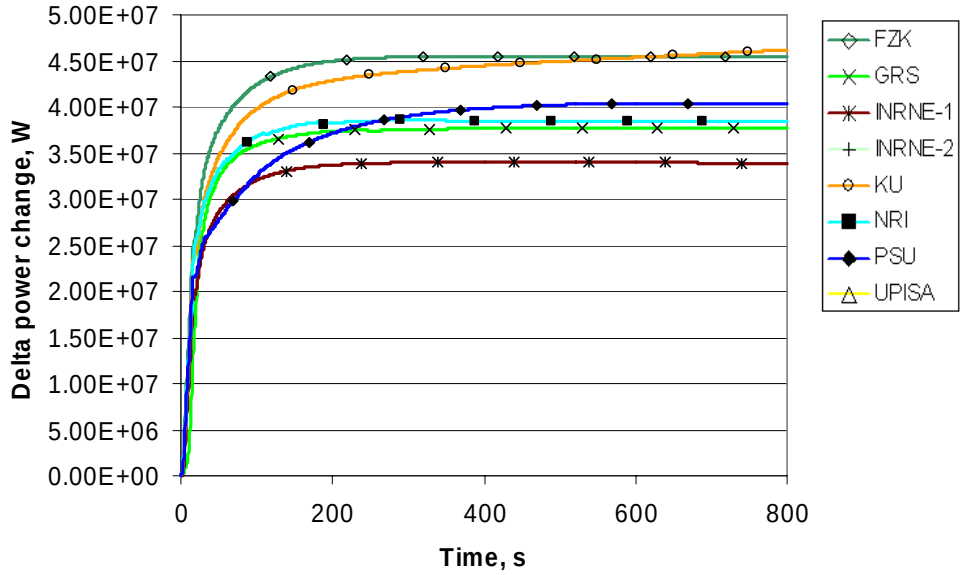

Table 4.27. Fission power initial value

Participant	Result, W
FZK	7.69E+08
GRS	7.64E+08
INRNE-1	7.71E+08
KI	7.65E+08
KU	7.42E+08
NRI	7.65E+08
PSU	7.65E+08

Figure 4.24. Total feedback reactivity during the transient

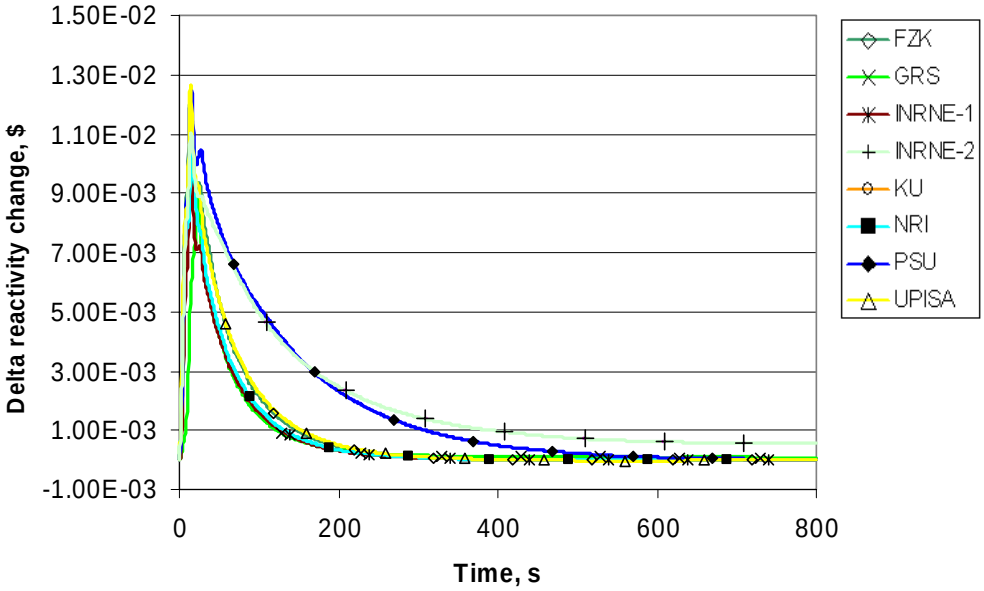

Figure 4.25. Core average fuel temperature change during the transient

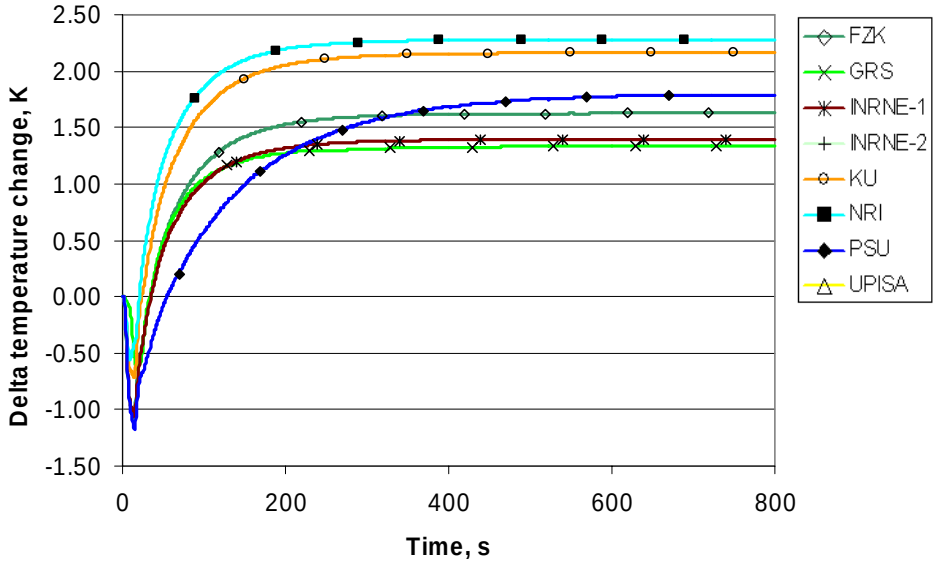

Table 4.28. Core average fuel temperature initial value

Participant	Result, K
FZK	651.94
GRS	661.48
INRNE-1	675.12
KU	660.64
NRI	680.16
PSU	659.13

Figure 4.26. Core average moderator temperature change during the transient

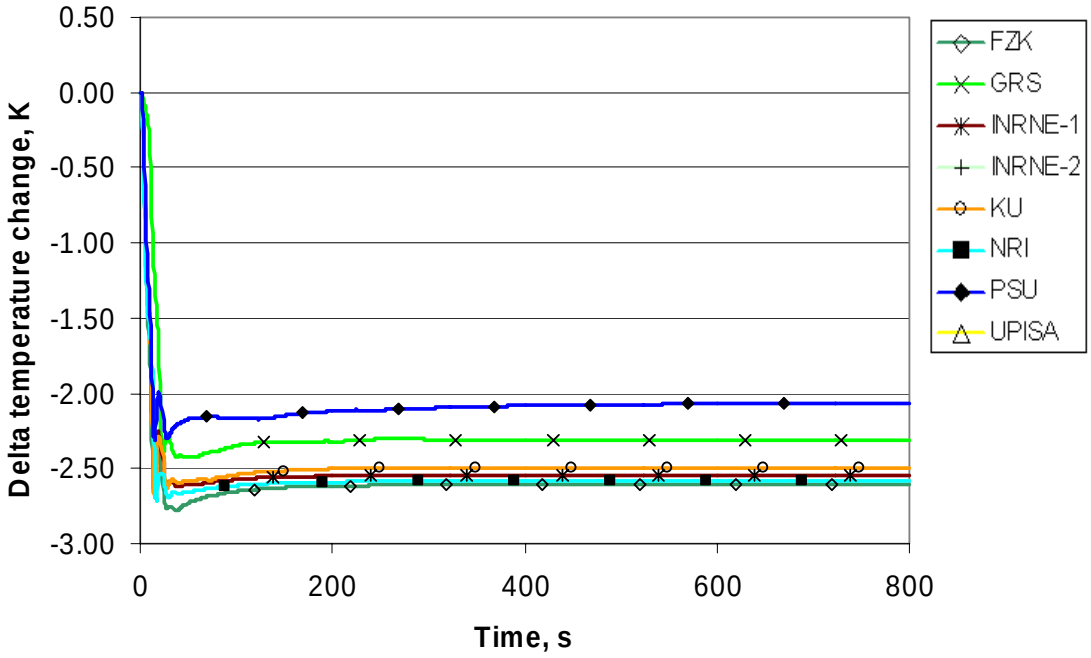

Table 4.29. Core average moderator temperature initial value

Participant	Result, K
FZK	562.19
GRS	560.91
INRNE-1	561.79
KU	562.26
NRI	562.01
PSU	561.08

Figure 4.27. Loop #1 mass flow rate change during the transient

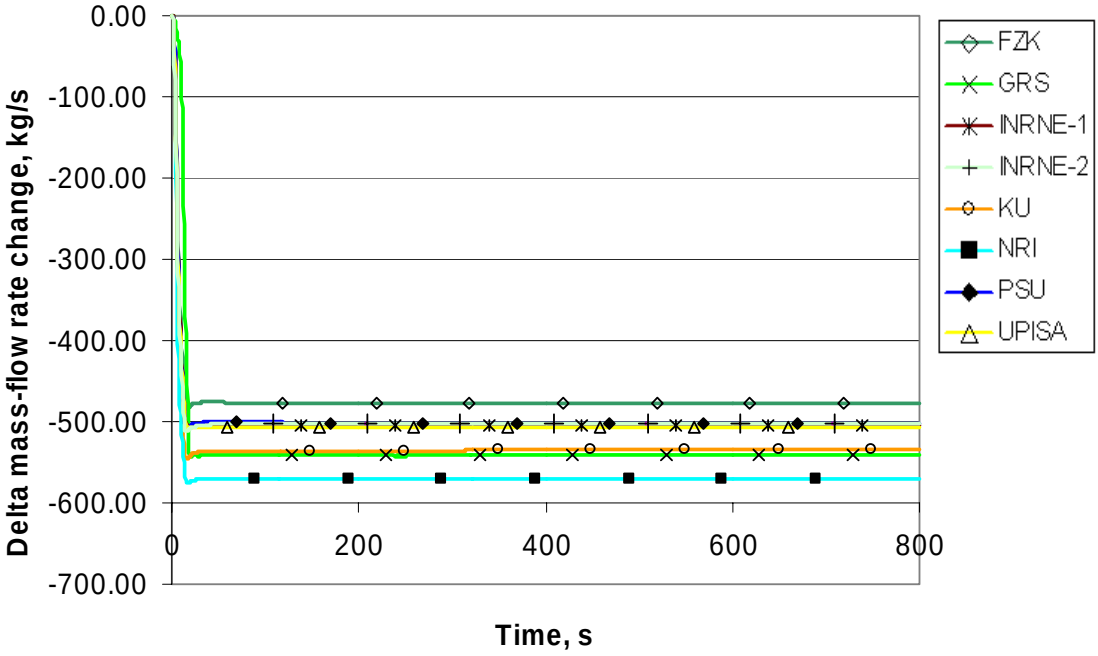

Figure 4.28. Loop #2 mass flow rate change during the transient

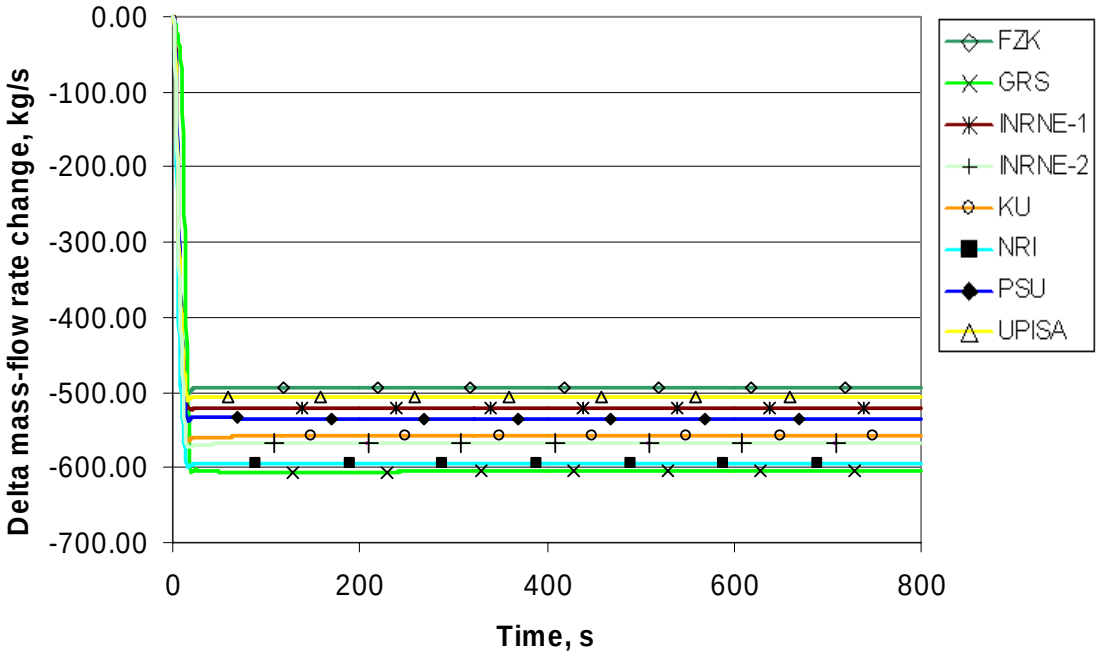

Figure 4.29. Loop #3 mass flow rate change during the transient

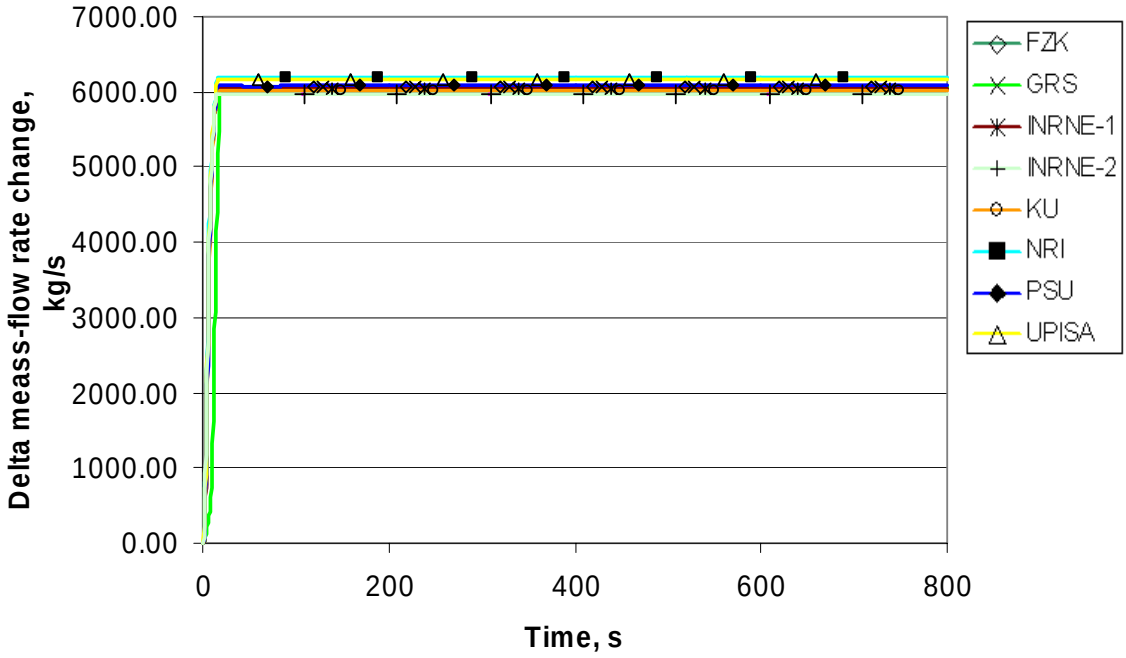

Figure 4.30. Loop #4 mass flow rate change during the transient

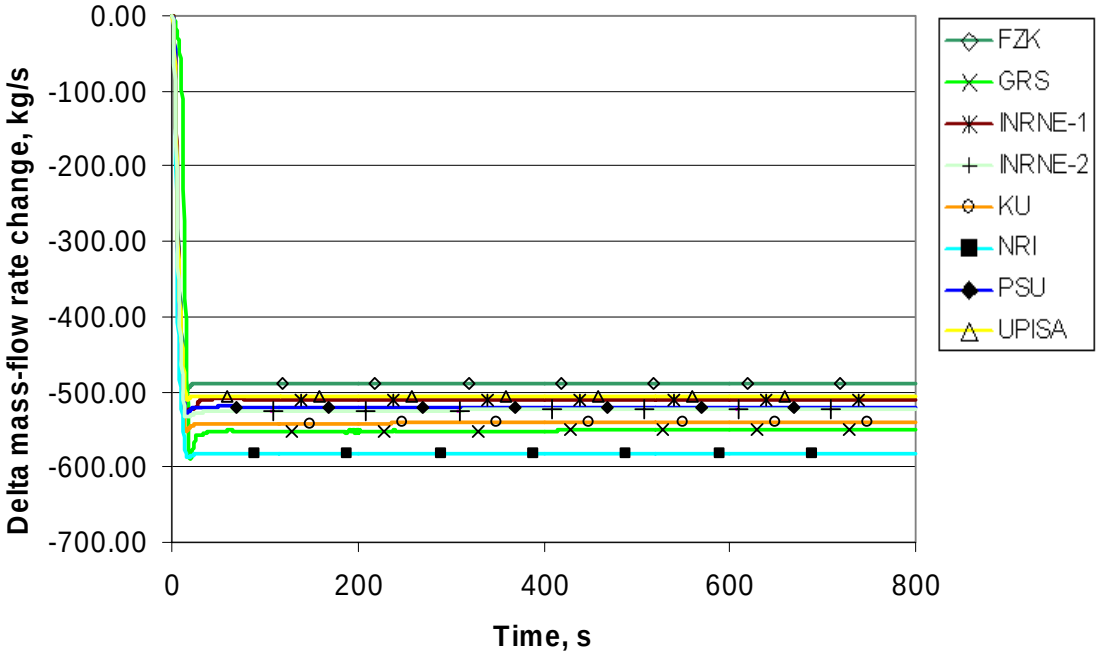

Chapter 5

CONCLUSION

The OECD/DOE/CEA V1000CT benchmark was developed to provide a validation basis for the new generation of best-estimate codes – coupled 3-D neutron kinetics thermal-hydraulic system codes. Based on previous experience, three benchmark exercises were defined, allowing for a consistent and comprehensive validation process. The purpose of Exercise 1 is to test the primary and secondary system model responses using a point kinetics simulation. This exercise enables participants to initialise and verify their thermal-hydraulics models before focusing on the main objective of the benchmark: the testing of coupling methodologies in terms of numerics, temporal and spatial mesh overlays. This benchmark was created to enable the determination of the applicability of the 3-D coupled thermal-hydraulics/neutron kinetics codes to safety analysis of VVER-1000 special transients. The benchmark is based on a real plant transient wherein one main coolant pump switches on while the other three pumps are in operation.

A detailed evaluation of the differences between the calculated results submitted by the participants and the plant-measured data are presented in Chapter 4. The analyses of the results of Exercise 1 show that the participants' results for each parameter are in good agreement. The explanation of some of the discrepancies in the participants' steady-state and transient results for Exercise 1 is based on the observed differences as reported in Table 4.1 and the answers to the questionnaire given in Appendix B. Some of these differences include the utilisation of the provided SG BC, MCP #3 rotor speed, and decay heat modelling as well as different vessel nodalisation and/or number of channels. The discrepancies of the predictions of power change during the transient reflect the corresponding discrepancies in prediction of the total reactivity change. The total reactivity change during the transient is determined by the Doppler and moderator temperature feedback effects. Since the DTC and MTC are provided for Exercise 1, the discrepancies arise from the differences in prediction of core average fuel temperature and core average moderator temperature time histories. The discrepancies in predictions of the fuel temperature arise from differences in modelling of the fuel rod (heat structure) component (for example the gas gap conductance model, nodalisation and the relation for obtaining the effective Doppler temperature), as reported in the participants' answers to the questionnaire.

Overall, the participants' results for each parameter are in good agreement. Exceptions include the primary pressure and the pressuriser's liquid level. The differences in these parameters were evaluated and the most probable reason is the lack or insufficient modelling of the make-up and let-down systems and the logic used to operate them. Another reason contributing to these deviations is the MCP's homologous curves provided in the specification (as discussed in Chapter 4).

Initially, the comparison for the cold and hot leg temperatures showed poor agreement between the calculated values and the plant data for most of the loops. This was due to the fact that all codes predicted the exact situation during the transient, while the plant data showed smoother variations of the parameters because of the time delay of the measurement system. In order to better compare the code predictions to the plant data, the benchmark team incorporated the time delay of the measurement

system into the participants' results. In each case, the updated participants' results are in reasonable agreement with the trend of the measured value. At the end of the transient all of the participants' results for all of the cold and hot legs are within the uncertainty band of the measurement system.

From the results presented in this report it can be concluded that all the codes are capable of modelling the transient "MCP switching on when the other three pumps are in operation" in a VVER-1000 system. There are deviations of the steady-state and transient results from the plant data but almost every compared parameter is within the measurement uncertainties.

Overall, this benchmark has been well accepted internationally, with nine organisations representing seven countries participating in the first exercise of Phase I of the benchmark. The results submitted by the participants for Exercise 1 were used to prepare code-to-code and code-to-plant data comparisons with subsequent statistical analyses. The results of this exercise enabled participants to initialise and verify their system models, which in turn is very important for conducting a correct assessment of the performance of the coupled codes in the next two exercises of Phase I of the benchmark.

REFERENCES

[1] Ivanov, K., P. Groudev, R. Gencheva and B. Ivanov, *Letter-Report on Kozloduy NPP Transient*, US DOE, September 2000.

[2] Ivanov, K. *et al*., *PWR MSLB Benchmark Volume 1: Final Specifications*, NEA/NSC/DOC(99)8, April 1999.

[3] Solis, J. *et al*., *Boiling Water Reactor Turbine Trip (TT) Benchmark Volume I: Final Specifications*, NEA/NSC/DOC(2001)1, June 2001.

[4] Ivanov, B., K. Ivanov, P. Groudev, M. Pavlova and V. Hadjiev, *VVER-1000 Coolant Transient Benchmark (V1000-CT) Phase I – Final Specification*, NEA/NSC/DOC(2002)6.

[5] Kuntz, R.F., G.F. Kasmala, J.H. Mahaffy, *Automated Code Assessment Program: Technique Selection and Mathematical Prescription*, Applied Research Laboratory, Pennsylvania State University, Letter Report 3 to US NRC, April 1998.

[6] M. Rajamäki, *TRAWA, A Transient Analysis Code for Water Reactors*, Revised edition, Espoo (1980), Technical Research Centre of Finland, Nuclear Engineering Laboratory, Report 24. 149 p + app. 31 p.

[7] Kyrki-Rajamäki, R., J. Miettinen, H. Räty and T. Vanttola, "Validation of SMATRA Accident Analysis Code Against Loviisa Plant Data", *Proc. of the 3rd International Symposium on Power Plant Transients*, 1992 ASME Winter Annual Meeting, Anaheim, CA, 8-13 November 1992. New York, NY: American Society of Mechanical Engineers (1992). FED-Vol. 140, pp. 153-162.

[8] Hämäläinen, R. Kyrki-Rajamäki, S. Mittag, S. Kliem, F.P. Weiss, S. Langenbuch, S. Danilin, J. Hadek and G. Hegyi, "Validation of Coupled Neutron Kinetic/Thermal-hydraulic Codes. Part 2: Analysis of a VVER-440 Transient (Loviisa-1)", *Annals of Nuclear Energy*, Vol. 29, pp. 255-269 (2002).

[9] Austregesilo, H., C. Bals, A. Hora, G. Lerchl, P. Romstedt, "ATHLET, Mod 2.0 Cycle A, Models and Methods", GRS-P-1/Vol. 4, Gesellschaft für Anlagen- und Reaktorsicherheit (GRS) mbH, Germany, October 2003.

[10] Bestion, D., *General Description of CATHARE 2 V1.3*, STR/LML/EM/94-265, CEA Grenoble (1994).

[11] The RELAP5 Development Team, *RELAP5/MOD3.2 Code Manual*, NUREG/CR-5535, INEL-95/0174, Vol. 1, August 1995.

[12] *RELAP5-3D Code Manuals: Volume I: Code Structure, System Models and Solution Methods; Volume II: User's Guide and Input Requirements; Volume IV: Models and Correlations; Volume V: User's Guidelines*, INEEL-EXT-98-00834, Revision 1.3a, February 2001.

[13] Schnurr, N.M., R.G. Steinke, V. Martinez and J.W. Spore, *TRAC-PF1/MOD2. Volume II: User's Guide*.

[14] Ivanov, K., *et al*., "Features and Performance of a Coupled Three Dimensional Thermal-Hydraulics/Kinetics Code TRAC-PF1/NEM PWR Analysis Code", *Ann. Nucl. Energy*, 26, 1407 (1999).

Appendix A

DESCRIPTION OF CODES

ATHLET (GRS, KI and NRI)

The thermal-hydraulic computer code ATHLET (Analysis of THermal-hydraulics of LEaks and Transients) is being developed by the Gesellschaft für Anlagen- und Reaktorsicherheit (GRS) for the analysis of anticipated and abnormal plant transients, small and intermediate leaks as well as large breaks in light water reactors [9]. The aim of the code development is to cover the whole spectrum of design basis and beyond design basis accidents (without core degradation) for PWRs and BWRs with only one code. The main code features are: advanced thermal-hydraulics, modular code architecture, separation between physical models and numerical methods, pre- and post-processing tools and portability.

The code development is accompanied by a systematic and comprehensive validation programme. A large number of integral experiments and separate effect tests, including the major International Standard Problems, have been calculated by GRS and by independent organisations. The range of applicability has been extended to the Russian reactor types VVER and RBMK in co-operation with foreign partner organisations.

ATHLET is being applied by numerous institutions in Germany and abroad; its development and validation are sponsored by the German Federal Ministry of Economics and Labour (BMWA).

CATHARE2 v1.3 (INRNE-2)

CATHARE2 is a best-estimate code for thermal-hydraulic reactor safety studies covering the domain of large breaks, small breaks and transients. It was developed in CEA Grenoble in the framework of a CEA, EDF and FRAMATOME joint effort. Successive versions are released to users. The current version V2.5 includes a 3-D coarse-mesh module. This summary presents CATHARE2 V1.3L_1 [10], used to solve the benchmark problem. The main characteristics of the code are:

- a modular structure with the possibility to represent any reactor and test facility by assembling modules and sub-modules;
- the two-fluid model which is used in all main modules;
- time discretisation is fully implicit for the 1-D module, and the space discretisation uses the staggered mesh and the donor cell principle;
- the constitutive relations are established mainly on the basis of an extensive experimental support programme;
- each version is carefully assessed following a two-step procedure: qualification of the closure relations on a large separate effect test matrix, and verification of the overall code behaviour on an integral test matrix.

Every module is able to describe the mechanical and thermal non-equilibrium which may be encountered in various components of PWR circuits. Advanced modelling of breaks is possible.

CATHARE may be used for several types of PWR including western designs and VVER. The experimental program carried out for assessment includes separate effect tests, component tests and integral tests. The qualification matrix includes experiments relative to VVER such as GP horizontal SG, CCFL and re-flooding. All the existing integral test facilities with horizontal steam generators (PACTEL, PMK and PSB) were used for the assessment. The code has been tested in multi-1-D calculations of VVER-1000 plant experiments, including the OECD benchmarks on coolant mixing tests and main coolant pump start-up.

RELAP5 (FZK, INRNE-1 and UPISA)

The RELAP5/MOD3.2 computer code is a light water reactor (LWR) transient analysis code developed for the US Nuclear Regulatory Commission (NRC) [11]. Code uses include analyses required to support rulemaking, licensing audit calculations, evaluation of accident mitigation strategies, evaluation of operator guidelines and experiment planning analysis. RELAP5 has also been used as the basis for a nuclear plant analyser. Specific applications have included simulations of transients in LWR systems such as loss of coolant, anticipated transients without scram (ATWS), and operational transients such as loss of feedwater, loss of off-site power, station blackout and turbine trip. RELAP5 is a highly generic code that, in addition to calculating the behaviour of a reactor coolant system during a transient, can be used for simulation of a wide variety of hydraulic and thermal transients in both nuclear and non-nuclear systems involving mixtures of steam, water, non-condensable and solute.

The purpose of the RELAP5/MOD3.2 development programme was to develop a code version suitable for the analysis of all transients and postulated accidents in LWR systems, including both large and small break loss-of-coolant accidents (LOCAs) as well as the full range of operational transients.

The RELAP5/MOD3.2 code is based on a non-homogeneous and non-equilibrium model for the two-phase system that is solved by a fast, partially implicit numerical scheme to permit economical calculation of system transients. The objective of the RELAP5 development effort from the outset was to produce a code that included important first-order effects necessary for accurate prediction of system transients but that was sufficiently simple and cost effective to make possible parametric or sensitivity studies.

The code includes many generic component models from which general systems can be simulated. The component models include pumps, valves, pipes, heat releasing or absorbing structures, reactor point kinetics, electric heaters, jet pumps, turbines, separators, accumulators and control system components. In addition, special process models are included for effects such as form loss, flow at an abrupt area change, branching, choked flow, boron tracking and non-condensable gas transport.

The system mathematical models are coupled into an efficient code structure. The code includes extensive input checking capability to help the user discover input errors and inconsistencies. Also included are free-format input, re-start, re-nodalisation and variable output edit features.

The RELAP5/MOD3.2 hydrodynamic model is a one-dimensional, transient, two-fluid model for flow of a two-phase steam-water mixture that can contain non-condensable components in the steam phase and/or a soluble component in the water phase.

The RELAP5/MOD3.2 reactor point kinetics model is the simplest model that can be used to compute the transient behaviour of the neutron fission power in a nuclear reactor. This model is the same as in RELAP5-3D.

RELAP5-3D (KU and ORNL)

The RELAP5-3D code [12] was developed at the Idaho National Engineering and Environmental Laboratory under the sponsorship of the US Nuclear Regulatory Commission, the US Department of Energy and a consortium of several countries and domestic organisations that were members of the International Code Assessment and Applications Program for best-estimate transient simulation of light water reactor coolant systems during postulated accidents. The code models the coupled behaviour of the reactor coolant system and the core for loss-of-coolant accidents and operational transients.

RELAP5-3D, the latest in the series of RELAP5 codes, is a highly generic code that, in addition to calculating the behaviour of a reactor coolant system during a transient, can be used for simulation of a wide variety of hydraulic and thermal transients in both nuclear and non-nuclear systems. The most prominent attribute that distinguishes the RELAP5-3D code from the previous versions is the fully integrated, multi-dimensional thermal-hydraulic and kinetic modelling capability. This removes any restrictions on the applicability of the code to the full range of postulated reactor accidents.

The RELAP5-3D hydrodynamic model is a transient, two-fluid model for the flow of a two-phase vapour/gas-liquid mixture that can contain non-condensable components in the vapour/gas phase and/or a soluble component in the liquid phase. Both one-dimensional and multi-dimensional hydrodynamic models are included in the code. The RELAP5-3D hydrodynamic model contains several options for invoking simpler hydrodynamic models. These include homogeneous flow, thermal equilibrium and frictionless flow models. These options can be used independently or in combination. The two-fluid equations of motion that are used as the basis for the RELAP5-3D hydrodynamic model are formulated in terms of volume and time-averaged parameters of the flow. Phenomena that depend upon transverse gradients, i.e. friction and heat transfer, are formulated in terms of the bulk properties using empirical transfer coefficient formulations. In situations where transverse gradients cannot be represented within the framework of empirical transfer coefficients, i.e. sub-cooled boiling, additional models specially developed for the particular situation are employed.

RELAP5-3D heat structure models permit the calculation of the heat transferred across solid boundaries of hydrodynamic volumes. Modelling capabilities of heat structures are general and include fuel pins or plates with nuclear or electrical heating, heat transfer across steam generator tubes, and heat transfer from pipe and vessel walls. Temperatures and heat transfer rates are computed from the one-dimensional form of the transient heat conduction equation for non-re-flood and from the two-dimensional form of the transient heat conduction equation for re-flood. For one-dimensional heat conduction, heat structures are represented using rectangular, cylindrical or spherical geometry. Surface multipliers are used to convert the unit surface of the one-dimensional calculation to the actual surface of the heat structure. Temperature-dependent thermal conductivities and volumetric heat capacities are provided in tabular or functional form either from built-in or user-supplied data. Finite differences are used to advance the heat conduction solutions. Each mesh interval may contain different mesh spacing, a different material or both. The spatial dependence of the internal heat source may vary over each mesh interval. The time dependence of the heat source can be obtained from reactor kinetics, one of several tables of power versus time or a control system variable. Boundary conditions include symmetry or insulated conditions, a correlation package, tables of surface temperature versus time, heat transfer rate versus time, and heat transfer coefficient versus time or surface temperature. The heat transfer correlation package can be used for heat structure surfaces connected to hydrodynamic volumes, and

contains correlations for convective, nucleate boiling, transition boiling and film boiling heat transfer from the wall to fluid and reverse transfer from fluid to wall, including condensation. A two-dimensional conduction scheme is used in the re-flood model for cylindrical or rectangular heat structures.

The RELAP5-3D gap conductance model defines an effective gap conductivity based on a simplified deformation model. The model employs three assumptions as follows: (a) the fuel-to-cladding radiation heat transfer, which only contributes significantly to the gap conductivity under the conditions of cladding ballooning, is neglected unless the cladding deformation model is activated; (b) minimum gap size is limited such that the maximum effective gap conductivity is about the same order as that of metals; (c) the direct contact of the fuel pellet and the cladding is not explicitly considered.

There are two options for the computation of the reactor power in the RELAP5-3D code. The first option is the point reactor kinetics model developed at the INEEL. The second is a multi-dimensional neutron kinetics model developed at North Carolina State University.

The reactor point kinetics model is the simplest model that can be used to compute the transient behaviour of the neutron fission power in a nuclear reactor. The power is computed employing the space-independent or point kinetics approximation, which assumes that power can be separated into space and time functions. This approximation is adequate for cases in which the space distribution remains nearly constant. The point reactor kinetics model computes both the immediate (prompt and delayed neutrons) fission power and the power from decay of fission products. Decay power is generated as the fission products undergo radioactive decay. The user can select the decay power model based on the approximate implementation of the 1973 ANS Proposed Standard, the exact implementation of the 1979 ANSI/ANS Standard or the exact implementation of the 1994 ANSI/ANS Standard. Either separable or tabular models can be selected for reactivity feedback in point reactor kinetics.

The multi-dimensional neutron kinetics model was developed to allow the user to model reactor transients where the spatial distribution of the neutron flux changes with time. The neutron kinetics model uses the few-group neutron diffusion equations. Two or four energy groups can be utilised, with all groups being thermal groups (i.e. upscatter exits) if desired. Core geometries modelled include Cartesian and hexagonal. Three-, two- and one-dimensional models can be used. Various core symmetry options are available, including quarter, half and full core for Cartesian geometry and one-sixth, one-third and full core for hexagonal geometry. Zero flux, non-re-entrant current, reflective and cyclic boundary conditions are treated. The few-group neutron diffusion equations are spatially discretised with the Nodal Expansion Method (NEM). Quartic or quadratic polynomial expansions for the transverse integrated fluxes are employed for Cartesian or hexagonal geometries, respectively. Transverse leakage terms are represented by a quadratic polynomial or constant for Cartesian or hexagonal geometry, respectively. Discontinuity factors (DFs) are utilised to correct for homogenisation errors. Transient problems utilise a user-specified number of delayed neutron precursor groups. The neutron kinetics subroutines require as input the neutron cross-sections in the computational nodes of the kinetics mesh. A neutron cross-section model has been implemented that allows the neutron cross-sections to be parameterised as functions heat structure temperatures, fluid void fraction or fluid density, poison concentration and fluid temperatures. A flexible coupling scheme between the neutron kinetics mesh and the thermal-hydraulics mesh has been developed to minimise the input data needed to specify the neutron cross-sections in terms of thermal-hydraulic variables. A control rod model has been implemented so that the effect of the initial position and subsequent movement of the control rods during transients may be taken into account in the computation of the neutron cross-sections.

TRAC-PF1/NEM (PSU)

The Transient Reactor Analysis Code (TRAC) is an advanced best-estimate system code for analysing light water reactor (LWR) accidents. This code was developed at the Los Alamos National Laboratory under the sponsorship of the Reactor Safety Research Division of the US Nuclear Regulatory Commission (NRC) [13]. The code has the following features: a one- or three-dimensional treatment of the pressure vessel and its associated internals, a two-fluid non-equilibrium hydrodynamics model with a non-condensable gas field and a solute tracking, a flow-regime-dependant constitutive equation treatment, an optional re-flood tracking capability for bottom-flood and falling-film quench fronts and consistent treatment of entire accident sequences including the generation of consistent initial conditions.

TRAC is a component-oriented code. Input data cards define the components in a calculation. The available components allow the user to model virtually any PWR design or experimental configuration. Included components are accumulator, break, fill, heat structure, pipe, plenum, pressuriser, pump, steam generator, tee, turbine, valve and vessel with associated internals (downcomer, lower plenum, core, upper plenum, etc.).

Variable dimensions can be used to represent fluid dynamics. A three-dimensional (r,θ,z) flow calculation can be modelled within the reactor vessel. Multi-dimensional plenum and core flow effects and upper plenum pool formation and core penetration can be treated directly. The flow within the loop components is treated in one dimension to allow for an accurate calculation of the complex multi-dimensional flow patterns inside the reactor vessel.

A full two-fluid (six equations) hydrodynamic model describes the steam/water flow, thereby allowing important phenomena such as counter current flow to be treated explicitly. A seventh field equation (mass balance) describes a non-condensable gas field and an eight-field equation tracks the solutes in the liquid. The thermal-hydraulic equations describe the transfer of mass, energy and momentum between the steam/water phases and the interaction of these phases with the heat flow from the system structures.

TRAC-PF1 incorporates detailed heat transfer analyses of the vessel and the loop components. The code includes a two-dimensional (r,z) treatment of fuel rod heat conduction with dynamic fine-mesh rezoning to resolve both bottom-flood and falling-film quench fronts. TRAC-PF1 calculates the heat transfer from the fuel rods and other system structures using flow regime-dependant heat-transfer coefficients obtained from a generalised boiling curve based on a combination of local conditions and history effects.

The primary energy source for a nuclear reactor power plant is the reactor core. TRAC allows the user to model the power generation in the reactor core in several ways: a constant power, a power specified from a table and a point reactor kinetics with a reactivity feedback. The latter cases can be run with the reactor core at a constant, user-specified trip power until a user-specified trip occurs.

The code determines the core power by either of the following two methods. In the first method, the user specifies power to be a constant or defined by a power table supplied through the input. The table is a function of a system signal variable parameter or a control block output signal parameter. Linear interpolation determines the values between entries in the table. Power determination can be trip-controlled by evaluating the power table when the controlling trip is ON and by holding the power constant when the trip is OFF. In the second method, the user determines power from the solution of the point kinetics equations. These equations specify the time behaviour of the core power level with the neutronic reactivity (the sum of programmed reactivity and feedback reactivity) as the driving parameter.

The point kinetics equations are a coupled set of first-order differential equations defining the total thermal power and the delayed neutron precursor concentrations as a function of time. In our analysis we obtain the power by solving the point reactor kinetics equations.

Currently PSU, in particular the Reactor Dynamics and Fuel Management Group (RDFMG), uses a modified version of the code TRAC-PF1/MOD2 version 5.4 [14]. Version 5.4 incorporates a one-dimensional decay heat model that dynamically computes the decay heat axial shape during the transient. The 3-D thermal-hydraulics models provide the necessary local environment conditions surrounding the fuel rods.

Appendix B

ANSWERS TO THE EXERCISE 1 QUESTIONNAIRE

FZK

I. Primary system modelling

1. *Vessel thermal-hydraulic (T-H) model and nodalisation (1-D, 3-D and number of T-H channels or cells). How are the channels/T-H cells chosen?*

   A 1-D model of the RPV is realised with a total of 25 T-H fluid channels and 19 axial layers.

2. *How the mixing is modelled?*

   A full coolant mixing in the lower and upper plenum was considered.

3. *How are the lower plenum and downcomer modelled?*

   The downcomer is represented by 4 parallel and equal channels (one channel per loop) connected to each other by cross-flow junctions along all 13 axial elevations. On the contrary the lower plenum is represented by a stack of two volumes, in which the coolant coming through the four cold legs get mixed.

4. *How are the upper head and the upper plenum modelled?*

   The inner zone of the upper plenum is represented by a stack of four volumes. The core outlet flow gets mixed with the bypass flow in the first volume above the core. The outer circular ring is represented by four equal volumes (one per loop). The volume belonging to loop #3 is connected with the volume of loop #2 and of loop #4 by a cross-flow junction CFD studies. The form loss coefficients of these cross-flow junctions were adjusted based on CFD simulations of the detailed flow conditions in the upper plenum for the stationary plant state. The upper head is modelled by two stacks of volumes only.

5. *How are the make-up and let-down systems modelled and what is the logic used?*

   The make-up and let-down systems are modelled by means of a time-dependent volume (source), time-dependent junction, a branch and four junctions that inject water into the cold legs just before the pumps. The prescribed mass flow rate (according to the logic defined in specifications) for both steady-state and transient conditions is assured by means of a control system and trips. The let-down system extracts water from the primary system by means of two junctions (cold legs of loop #2 and #3, volumes close to the RPV).

6. *How are the pressuriser's heaters modelled?*

   The pressuriser is modelled by a stack of four volumes (bottom part, central section, upper and uppermost volume) where the central volume consists of five axial elevations. The four groups of heaters, each one with different power, are connected with the second axial node of the central PZR-volume. The heater switch-off and switch-on logic described in the specifications is implemented in the model taking into account the pressure set-points.

7. *Are you using the pump head characteristics given in the specification?*

   Yes.

8. *Are using the MCP #3 rotor speed boundary conditions?*

   Yes.

II. Thermal-hydraulic core model

1. *Core thermal-hydraulic (T-H) model and nodalisation (1-D, 3-D and number of T-H channels or cells). How are the channels/T-H cells chosen?*

   The core T-H model is a 1-D model consisting of one average channel with 12 axial elevations, 10 in the core region and one for the lower and upper axial reflector, respectively.

2. *Number of heat structures (fuel rods) modelled?*

   Here also, only one average heat structure representing all fuel pins in the core is considered.

3. *What is the radial and axial heat structure (fuel rod) nodalisation?*

   For the heat structure 10 axial elevations are considered. In radial direction the representative heat structure consists of 10 nodes, 6 of them within the fuel pellet and 4 in the cladding region. A central hole and a gap are also considered in the model.

4. *What is the relation used for Doppler temperature?*

   The one defined in the specification was used.

5. *Used correlations for fuel properties vs. temperature?*

   The relations given in the specifications were used.

III. Secondary system

1. *Are you using steam generator (SG) feedwater boundary condition?*

   No.

2. *Are you using SG exit pressure boundary condition?*

   No.

IV. General

1. *Deviations from the updated Final Specifications?*

   The complete secondary system (steam line, common header, turbine, condenser, SRV, steam dump valves, feedwater system, etc.) is modelled so that the secondary pressure and the SG secondary side water level in each loop meets reasonably well the values given in the specifications within the error band.

2. *User assumptions?*

   None.

3. *Specific features of the codes used?*

   None.

GRS

I. Primary system modelling

1. *Vessel thermal-hydraulic (T-H) model and nodalisation (1-D, 3-D and number of T-H channels or cells). How are the channels/T-H cells chosen?*

   The VVER-1000 NPP model for the ATHLET code consists of a reactor pressure vessel model and four loops for the primary side. Each loop consists of the hot leg, the horizontal steam generator, the cold leg with the main coolant pump. The pressuriser is connected to the unaffected loop #4.

   In the ATHLET model the flow through the reactor pressure vessel is described by four parallel downcomers, a lower plenum, a core region with a single thermal-hydraulic channel with one fuel rod and a parallel bypass channel, the upper plenum and the reactor head. The core channel and the bypass channel are divided into 10 axial nodes.

2. *How the mixing is modelled?*

   Mixing is taken into account in the upper plenum. Cross-flow is only considered in the upper plenum between the inner and outer ring.

3. *How are the lower plenum and downcomer modelled?*

   The downcomer is modelled by four flow paths. The coolant flows into the lowest volume of the lower plenum and then upwards through three further axial volumes.

4. *How are the upper head and the upper plenum modelled?*

   The upper head is modelled by two volumes. The upper plenum consists of four volumes in four axial levels. The flow through the core and reflector is collected in the lower volume of the upper plenum. The following two volumes on higher levels are divided into four parallel flow paths and in addition the upper volume of this part in the flow direction is modelled with two radial zones. The inner ring models the part above the core with the shielding tube block and the space till the perforated barrel. The outer ring includes the volume between the barrel and the nozzles. The two ring volumes are connected with radial junctions allowing radial flow.

5. *How are the make-up and let-down system modelled and what is the logic used?*

   The make-up system and the let-down system are not modelled. Therefore, the results of our calculation show a greater pressure decrease than in the measurement.

6. *How are the pressuriser's heaters modelled?*

   The heaters of the pressuriser are modelled as in *Table 5.4.5. Pressuriser heaters logic*, of the Specification described. The reset value of heater 2 was corrected from 15.60 MPa to 15.78 MPa, because the set value of this heater is specified as 15.60 MPa. Thus the set and reset values of the two heaters are the same.

7. *Are you using the pump head characteristics given in the specification?*

   We do not use the pump head specification. We use our own pump model for the VVER-1000 NPP.

8. *Are using the MCP #3 rotor speed boundary conditions?*

   The MCP #3 rotor speed boundary conditions are not used, but the rotor speed of our pump model is very similar to this boundary condition.

II. Thermal-hydraulic core model

1. *Core thermal-hydraulic (T-H) model and nodalisation (1-D, 3-D and number of T-H channels or cells). How are the channels/T-H cells chosen?*

   The reactor core is modelled by a single thermal-hydraulic channel and a parallel bypass channel. Each of the channels consists of 10 axial nodes. The bypass flow is about 4% of the flow through the core at the beginning of the transient.

2. *Number of heat structures (fuel rods) modelled?*

   One average fuel rod is considered in the thermal-hydraulic channel.

3. *What is the radial and axial heat structure (fuel rod) nodalisation?*

   The fuel rod also has 10 axial nodes. Two material zones, the fuel and the cladding, are treated. The core channel and the bypass channel are divided into 10 axial nodes. Cross-flow is only considered in the upper plenum between the inner and outer ring.

4. *What is the relation used for Doppler temperature?*

   The proposed relation of Chapter 3.3 in the Specification is not taken. The mean value of the fuel temperature for the 10 axial nodes in the 4 layers is determined and used for calculating the Doppler feedback.

5. *Used correlations for fuel properties vs. temperature?*

   The dependency of the material temperature for the specific heat capacity, the heat conductivity and the density of the fuel and the cladding is considered by tables.

III. Secondary system

1. *Are you using steam generator (SG) feedwater boundary condition?*

   Yes, we use the specified SG feedwater as boundary condition for the whole transient and for the 4 steam generators.

2. *Are you using SG exit pressure boundary condition?*

   Yes, we use the values of the four SGs exit pressure as boundary condition.

IV. General

1. *Deviations from the updated Final Specifications?*

   None.

2. *User assumptions?*

   None.

3. *Specific features of the codes used?*

   There are no further relevant deviations from the Specifications and specific features that should be mentioned.

INRNE-1

I. Primary system modelling

1. *Vessel thermal-hydraulic (T-H) model and nodalisation (1-D, 3-D and number of T-H channels or cells). How are the channels/T-H cells chosen?*

   The reactor vessel includes a downcomer, lower plenum and outlet plenum. Four inlet and outlet nozzles are modelled with connections between them to model the core bypass flow. The reactor vessel is divided into 10 layers. The cells are chosen symmetrical.

2. *How the mixing is modelled?*

   The mixing is modelled by cross-flow junction.

3. *How are the lower plenum and downcomer modelled?*

   The downcomer is modelled by annulus components. Four downcomer parts are divided into 13 layers with "mtpljun" type junctions between them. The lower plenum of the reactor vessel is connected with downcomers by cross-flow junctions. The down-mixing volume is modelled as a branch component and is connected with the reactor core by three junctions.

4. *How are the upper head and the upper plenum modelled?*

   The upper head and upper plenum are modelled by branch components. The upper plenum is presented as one volume.

5. *How are the make-up and let-down systems modelled and what is the logic used?*

   The logic used is that of the Specifications.

6. *How are the pressuriser's heaters modelled?*

   The pressuriser heaters are modelled as a four-group heat structure.

7. *Are you using the pump head characteristics given in the specification?*

   Yes.

8. *Are using the MCP #3 rotor speed boundary conditions?*

   Yes.

II. Thermal-hydraulic core model

1. *Core thermal-hydraulic (T-H) model and nodalisation (1-D, 3-D and number of T-H channels or cells). How are the channels/T-H cells chosen?*

   The core region is modelled by 3 parallel channels. The channels are chosen by core exit temperature at nominal operations.

2. *Number of heat structures (fuel rods) modelled?*

   The fuel rods are modelled as hot channel, average channel and bypass. Each channel is divided into 10 sub-volumes. The hot assembly channel (represented with 14 assemblies), the average core (represented with 149 assemblies) and the bypass channel.

3. *What is the radial and axial heat structure (fuel rod) nodalisation?*

   The fuel channels are divided in 8 axial volumes. Eight axial heat structures and 8 radial mesh points for cylindrical geometry type were used. Steady-state initialisation option 1 was chosen, whereby the steady-state initial condition temperatures are calculated by the code. The hole in the pellet is modelled by the left boundary co-ordinate.

4. *What is the relation used for Doppler temperature?*

   For Doppler temperature tables have been used.

5. *Used correlations for fuel properties vs. temperature?*

   None.

III. Secondary system

1. *Are you using steam generator (SG) feedwater boundary condition?*

   No.

2. *Are you using SG exit pressure boundary condition?*

   No.

IV. General

1. *Deviations from the updated Final Specifications?*

   None.

2. *User assumptions?*

   None.

3. *Specific features of the codes used?*

   Relap5/Mod3.2 (frozen version).

INRNE-2

I. Primary system modelling

1. *Vessel thermal-hydraulic (T-H) model and nodalisation (1-D, 3-D and number of T-H channels or cells). How are the channels/T-H cells chosen?*

   The CATHARE2 V1.3 model used four 1-D channels connected by cross-flows. Each RPV channel consists of the following elements: inlet volume, downcomer, lower plenum, core, core bypass, upper plenum and outlet volume. All channels are connected to the upper head. The number of T-H nodes in the vessel without the core is 68 ($6 \times 11 + 2$).

2. *How the mixing is modelled?*

   Cross-flow was modelled with horizontal junctions at the reactor inlet and outlet, and vertical junctions to adjacent sectors in the lower and upper plenums. Vessel mixing is governed by tuned local pressure drops. Tuning is achieved through adjustment of the flow resistance at horizontal cross-flow junctions and flow area in vertical junctions.

3. *How are the lower plenum and downcomer modelled?*

   The lower plenum was modelled by 12 volumes in 2 axial layers. The downcomer in each channel was described by an axial element with 4 nodes.

4. *How are the upper head and the upper plenum modelled?*

   The upper head was modelled by 2 axial layers with 1 node per layer. The upper plenum (upward flow part) was described by 12 volumes in 2 axial layers. The annular zone between the perforated ring of the block of shielding tubes and the perforated core barrel was modelled by 6 volumes. The annular outlet zone was modelled by 6 volumes.

5. *How are the make-up and let-down system modelled and what is the logic used?*

   Make-up system: continuous flow = 30 m^3/h (6.274 kg/s at 16.0 MPa, T = 287°C), flow per loop = 6.274/4 = 1.57 kg/s.*

   * If the pressuriser level decreases: 1 pump from 30 to 60 m^3/h for 60 s.

6. *How are the pressuriser's heaters modelled?*

   Heaters #3 and #4 were lumped together.

7. *Are you using the pump head characteristics given in the specification?*

   No, the characteristics were as given by Gydropress.

8. *Are using the MCP #3 rotor speed boundary conditions?*

   Yes.

II. Thermal-hydraulic core model

1. *Core thermal-hydraulic (T-H) model and nodalisation (1-D, 3-D and number of T-H channels or cells). How are the channels/T-H cells chosen?*

   Thermal-hydraulics: Multi 1-D channel model with 6 main channels and 6 bypass channels.

   Axial mesh: 6 nodes for the non-heated part (reflectors) and 10 nodes of 35.5 cm for the fuel, a total of 16 axial T-H nodes.

2. *Number of heat structures (fuel rods) modelled?*

   Six (6) heat structures.

3. *What is the radial and axial heat structure (fuel rod) nodalisation?*

   Radial mesh: 5 iso-volume nodes in the pellet.

4. *What is the relation used for Doppler temperature?*

   As specified.

5. *Used correlations for fuel properties vs. temperature?*

   Approximately as specified.

III. Secondary system

1. *Are you using steam generator (SG) feedwater boundary condition?*

   No.

2. *Are you using SG exit pressure boundary condition?*

   No.

IV. General

1. *Deviations from the updated Final Specifications?*

   Pump head characteristics were as given by Gydropress.

   Pressuriser heaters #3 and #4 were lumped together.

2. *User assumptions?*

   Time delays in the measured data were not modelled.

3. *Specific features of the codes used?*

   None.

KI

I. Primary system modelling

1. *Vessel thermal-hydraulic (T-H) model and nodalisation (1-D, 3-D and number of T-H channels or cells). How are the channels/T-H cells chosen?*

   See points I.3, I.4 and II.1.

2. *How the mixing is modelled?*

   Cross-connection elements with cross-flows between cells at the same levels.

3. *How are the lower plenum and downcomer modelled?*

   Six downcomers modelled with six parallel thermal-hydraulic channels (PTHC) with cross-flows (CF). Four of them are connected directly with the four cold legs and the remaining two model the volumes between the first and second legs and between the third and fourth ones. This type of description of the downcomers follows the asymmetrical cold legs' nozzle locations on the reactor vessel periphery. The angle between the fourth and first nozzles and also between the second and third nozzles is 55°, but the angle between the first and second nozzles and also between the third and fourth nozzles is 125°.

   Six lower plenums (first level) modelled with six PTHCs with CFs which describe the volume including the reactor bottom part till the perforated elliptical bottom plate and the nodalisation follows the azimuthal nodalisation of the downcomers.

   Seven lower plenums (second level) modelled with seven PTHCs with CFs which describe the volume between the perforated elliptical bottom plate and the fuel assembly support plate. The new – seventh – THC is the channel located in the centre part of the plenum.

4. *How are the upper head and the upper plenum modelled?*

   - Seven upper plenums (first level) modelled with seven PTHCs with CFs which describe the volume between the active core and the upper assembly fixing cotter.
   - Six PTHCs for the core bypass.
   - Seven upper plenums (second level) modelled with seven PTHCs with CFs which describe the volume between the lower and middle part of the shielding tubes block.
   - One THC for the volume between the middle and upper part of the shielding tubes block.
   - One THC for the volume between the upper part of the shielding tubes block and reactor head.
   - Six azimuthal PTHCs with CFs (at the height of the upper plenum – second level) modelling the volume between the shielding tubes block perforated frame and the perforated barrel walls.
   - Six azimuthal PTHCs with CFs (at the height of the upper plenum – second level) modelling the volume between the perforated barrel walls and the cylindrical reactor vessel walls.

5. *How are the make-up and let-down system modelled and what is the logic used?*

   With FILL-elements and real station logic.

6. *How are the pressuriser's heaters modelled?*

   With different heat slabs and real station logic.

7. *Are you using the pump head characteristics given in the specification?*

   Yes.

8. *Are using the MCP #3 rotor speed boundary conditions?*

   No.

II. Thermal-hydraulic core model

1. *Core thermal-hydraulic (T-H) model and nodalisation (1-D, 3-D and number of T-H channels or cells). How are the channels/T-H cells chosen?*

   Seven PTHCs with/without CFs in the active core. In the case of point kinetics calculations the number of the PTHC can be increased to 1:1 modelling (163 PTHCs).

2. *Number of heat structures (fuel rods) modelled?*

   Heat structures are assigned for all objects in core.

3. *What is the radial and axial heat structure (fuel rod) nodalisation?*

4. *What is the relation used for Doppler temperature?*

   Used characteristics given in the specification.

5. *Used correlations for fuel properties vs. temperature?*

   Used characteristics given in the specification.

III. Secondary system

1. *Are you using steam generator (SG) feedwater boundary condition?*

   No.

2. *Are you using SG exit pressure boundary condition?*

   No.

IV. General

1. *Deviations from the updated Final Specifications?*

   Practically none.

2. *User assumptions?*

   Real station logic for modelling the system has been used.

3. *Specific features of the codes used?*

   None.

KU

I. Primary system modelling

1. *Vessel thermal-hydraulic (T-H) model and nodalisation (1-D, 3-D and number of T-H channels or cells). How are the channels/T-H cells chosen?*

   3-D vessel thermal-hydraulic model was modelled by the following:

   - six-sector annular downcomer (six channels);
   - six-sector lower plenum (six channels);
   - 54-channel core (48 channels for core fuel assemblies + 6 channels for core bypass);
   - six-sector upper plenum (six channels);
   - six-sector upper head (six channels);

   Heat exchange of the coolant with reactor pressure vessel internals and environment are simulated by the corresponding heat structures.

2. *How the mixing is modelled?*

   The cross-flows are available between all adjacent sectors or corresponding hydraulic channels. In particular for cross-flows between fuel channels the quantity of assembly faces is taken into account: $S_{flow} = N \times 10 \times (D_1 - D_2) \times \Delta z$ is the flow area, where D_1 is the pitch between fuel pins, D_2 is the fuel pin diameter, N is the quantity of assembly faces and Δz is the z-mesh interval.

3. *How are the lower plenum and downcomer modelled?*

   Lower plenum and downcomer was modelled as six-sector 3-D components with cross-flows between adjacent sectors.

4. *How are the upper head and the upper plenum modelled?*

   Upper plenum and upper head was modelled as six-sector 3-D components with cross-flows between adjacent sectors.

5. *How are the make-up and let-down system modelled and what is the logic used?*

   Each train of the make-up and let-down systems is modelled by time-dependent volume, time-dependent junction, collector, piping, control valves. The logic for the system operation (for controllers) is simulated by flow tables that depend on the pressuriser level.

   In this RELAP5-3D Exercise 1 analysis these systems were used only in steady-state run, i.e. to have initial pressuriser level value 7.44 m. During transient these steady-state flow rates of make-up and let-down systems remained constant as plant data on their change during transient are absent in the specification and the value of pressuriser level change during transient (7.44-7.28 = 0.16 m) is comparable with specified uncertainty ±0.15 m.

6. *How are the pressuriser's heaters modelled?*

   To simulate operation of pressuriser heaters the corresponding heat structures are used. Heater power can be increased due to consequent switching-on of heater groups according to logic of specified *Table 5.4.5. Pressuriser heaters logic*. However, against the previous RELAP5-3D analysis, in this run this logic was changed. According to specified logic the group #1 (off at P > 15.78 MPa) and #2 (off at P > 15.6 MPa) should to continue to work, whereas according to the plant data the primary pressure has new stable value 15.53-15.54 MPa. Therefore heater groups #1 and #2 were switched off at achievement of primary pressure 15.54 MPa.

7. *Are you using the pump head characteristics given in the specification?*

   Yes. The homologous curves (edit for pump single phase table input and edit for pump two-phase table set input), given in Appendix A of the Specification, were used for MCP (GCN-195 M) modelling.

8. *Are using the MCP #3 rotor speed boundary conditions?*

   Yes. Data of *Table 5.4.2. MCP #3 rotor speed boundary conditions* were used for switching-on of MCP #3.

II. Thermal-hydraulic core model

1. *Core thermal-hydraulic (T-H) model and nodalisation (1-D, 3-D and number of T-H channels or cells). How are the channels/T-H cells chosen?*

   3-D core hydraulic model was modelled by 48 channels for core fuel assemblies and 6 channels for core bypass. Core is simulated as 9-ring model with the following subdivisions:

   - first ring simulates central fuel assembly (1/6 FA in each sector);
   - second ring simulates 6 FAs (1 FA in each sector);
   - third ring simulates 12 FAs (2 FA in each sector);
   - fourth ring simulates 18 FAs (3 FA in each sector);
   - fifth ring simulates 24 FAs (4 FA in each sector);
   - sixth ring simulates 30 FAs (5 FA in each sector);
   - seventh ring simulates 36 FAs (6 FA in each sector);
   - eighth ring simulates 36 FAs (6 FA in each sector);
   - ninth ring simulates 6-sector core bypass.

2. *Number of heat structures (fuel rods) modelled?*

   3-D core thermal model with fixed power distribution of point kinetics approximation was modelled by 43 heat structures for fuel core (163 fuel assemblies) and 6 heat structures for 6-sector core bypass (see figure below):

   - heat structure #1 corresponds to central fuel assembly of first hydraulic ring;
   - heat structure #2 ÷ #7 correspond to 6 fuel assemblies of second hydraulic ring;
   - heat structure #8 ÷ #13 correspond to 12 fuel assemblies of third hydraulic ring;
   - heat structure #14 ÷ #19 correspond to 18 fuel assemblies of fourth hydraulic ring;
   - heat structure #20 ÷ #25 correspond to 24 fuel assemblies of fifth hydraulic ring;
   - heat structure #26 ÷ #31 correspond to 30 fuel assemblies of sixth hydraulic ring;
   - heat structure #32 ÷ #37 correspond to 36 fuel assemblies of seventh hydraulic ring;
   - heat structure #38 ÷ #43 correspond to 36 fuel assemblies of eighth hydraulic ring;
   - heat structure #44 ÷ #49 correspond to 6 sectors of core bypass;

   For fixed power distribution of point kinetics approximation the power distributions given in *Figure 5.3.1. Initial HP radial power distribution* and *Figure 5.3.2. Initial HP core average axial relative power distribution* were used.

3. *What is the radial and axial heat structure (fuel rod) nodalisation?*

   The axial heat structure nodalisation of fuel rod has 10 axial layers with same axial mesh intervals (0.355 m) and same following radial heat structure layout.

4. *What is the relation used for Doppler temperature?*

   In reactivity feedback calculations the Doppler temperature is fuel region averaged temperature, i.e. volume averaged temperature computation of fuel pin heat structure (see RELAP5-3D heat structure layout above), in which the temperatures of gas gap and cladding regions are excluded.

5. *Used correlations for fuel properties vs. temperature?*

   The used thermal conductivity and volumetric heat capacity of uranium dioxide (UO_2) versus temperature are data of *Table 3.3.1. Properties of fuel* of the Specification.

III. Secondary system

1. *Are you using steam generator (SG) feedwater boundary condition?*

   No. This SG feedwater boundary condition was obtained by run, which used full coolant mixing from different loops. Therefore using both specified SG feedwater boundary condition

and specified SG exit pressure boundary condition we will have an insufficiently exact description of the plant data for SG water levels during the transient (Tables C.2-C.4 of Appendix C of the Specification) in the RELAP5-3D model.

2. *Are you using SG exit pressure boundary condition?*

   Yes. Data of *Table 5.4.4. Steam generators pressure boundary conditions* were used in RELAP5-3D runs.

IV. General

1. *Deviations from the updated Final Specifications?*

   Against the previous KU RELAP5-3D analysis, in this analysis the pressuriser heaters logic specified in Table 5.4.5 was changed. According to this specified logic groups #1 (off at P > 15.78 MPa) and #2 (off at P > 15.6 MPa) should continue to work and RELAP5-3D primary pressure continues to be increased, whereas according to the plant data the primary pressure has a new stable value 15.53-15.54 MPa. For this reason the heater groups #1 and #2 were switched off at achievement of primary pressure 15.54 MPa.

   The SG feedwater boundary condition were not used as this SG feedwater boundary condition was obtained by run, which used full coolant mixing from different loops. Therefore using both specified SG feedwater boundary condition and specified SG exit pressure boundary condition we have an insufficiently exact description of the plant data for SG water levels during the transient (Tables C.2-C.4 in Appendix C of the Specification) in the RELAP5-3D model. For this reason the SG feedwater boundary conditions were changed so as to describe SG water levels during the transient as precisely as possible.

2. *User assumptions?*

   None.

3. *Specific features of the codes used?*

   None.

NRI

I. Primary system modelling

1. *Vessel thermal-hydraulic (T-H) model and nodalisation (1-D, 3-D and number of T-H channels or cells). How are the channels/T-H cells chosen?*

   Vessel nodalisation: 14 axial layers – 3 lower plenums, 5 core sub-volumes, 3 upper plenums (1 is divided into 2 sub-volumes), 1 head volume (divided into 2 sub-volumes).

   11 channels – 4 downcommers, 2 fuel channels, 1 core bypass, 1 lower plenum, 2 upper plenums, 1 head.

2. *How the mixing is modelled?*

   There are simulated by cross-connections between 4 downcomers. The downcomers are entering into one lower plenum PV-LP-1. Cross-connections between fuel channels are also simulated. The detailed figure of reactor vessel nodalisation and mixing is presented in Figure 2 of the presentation: J. Hádek, R. Meca, F. Lahovský, *NRI Řež Solution of V1000CT-1 Benchmark*, V1000-CT – 3rd Workshop, Garching, Germany, 4-5 April 2005.

3. *How are the lower plenum and downcomer modelled?*

   Three lower plenums (LP-1, LP-2 and LP-3) and four downcomers (PV-DC-1, PV-DC-2, PV-DC-3 and PV-DC-4) are modelled.

   For more detailed information see: J. Hádek, R. Meca, F. Lahovský, *NRI Řež Solution of V1000CT-1 Benchmark*, V1000-CT – 3rd Workshop, Garching, Germany, 4-5 April 2005.

4. *How are the upper head and the upper plenum modelled?*

   One upper head (PV-UH) and five upper plenums (PV-UP-1, PV-UP-2, PV-UP-3, PV-UP-4 and PV-UP-5) are modelled. Cross-connection between upper plenums PV-UP-1 and PV-UP-2 and PV-UP-3 and PV-UP-4 are modelled.

   For more detailed information see: J. Hádek, R. Meca, F. Lahovský, *NRI Řež Solution of V1000CT-1 Benchmark*, V1000-CT – 3rd Workshop, Garching, Germany, 4-5 April 2005.

5. *How are the make-up and let-down system modelled and what is the logic used?*

   Make-up and let-down systems are modelled with steady-state mass flow rate of 9.19 kg/s during the transient.

6. *How are the pressuriser's heaters modelled?*

   The pressuriser heaters power and heater logic corresponds exactly to the Final Specification.

7. *Are you using the pump head characteristics given in the specification?*

   No.

8. *Are using the MCP #3 rotor speed boundary conditions?*

   Yes.

II. Thermal-hydraulic core model

1. *Core thermal-hydraulic (T-H) model and nodalisation (1-D, 3-D and number of T-H channels or cells). How are the channels/T-H cells chosen?*

   The reactor core is divided into two parts PV-COR-IN and PV-COR-OUT. The inner part of core PV-COR-IN simulates 109 fuel assemblies. The outer part of core PV-COR-OUT simulates the outer part of the core with 54 fuel assemblies.

2. *Number of heat structures (fuel rods) modelled?*

   One type of heat structure (fuel rod) is modelled.

3. *What is the radial and axial heat structure (fuel rod) nodalisation?*

   In the radial direction the fuel rod (fuel pin) is divided into 4 layers for fuel and 2 layers for cladding.

   In the global nodalisation, the coolant channels PV-COR-IN and PV-COR-OUT containing fuel rods are divided into 5 axial layers. Each layer in the fuel rod is further divided into 5 axial layers. The fuel rod is thus divided into 25 axial layers.

4. *What is the relation used for Doppler temperature?*

   The average fuel temperature in the fuel rod segment is used.

5. *Used correlations for fuel properties vs. temperature?*

   λ, cp and ρ can be read in for every material zone as constant value or as a function of temperature, or they can be determined by correlations implemented in HECU. Correlations for the following materials are available:

   UO_2 fuel, valid between 260 and 2 750°C. For this temperature region, a constant density of 10 350 kg/m^3 is assumed:

$$c_p = c_0 + c_1 T + c_2 T^2 + c_3 T^3 + c_4 T^4$$

$$\lambda = \lambda_0/(T_k + 169.6) + \lambda_3 T_k^3$$

   where:

$$c_0 = 1.7419574 \times 10^2,\ c_1 = 6.1641512 \times 10^{-1},\ c_2 = -8.4878631 \times 10^{-4},$$
$$c_3 = 4.4559800 \times 10^{-7},\ c_4 = -7.0845012 \times 10^{-11},\ \lambda_0 = 3.8722385 \times 10^3,$$
$$\lambda_3 = 4.7120721 \times 10^{-11} \text{ and } T_k = T + 273.15,\ T \text{ in } °C$$

   Reference: Austregesilo, H., C. Bals, A. Hora, G. Lerchl, P. Romstedt, *ATHLET, Mod 2.0 Cycle A, Models and Methods*, GRS-P-1, Vol. 4.

III. Secondary system

1. *Are you using steam generator (SG) feedwater boundary condition?*

   Yes.

2. *Are you using SG exit pressure boundary condition?*

   Yes.

IV. General

1. *Deviations from the updated Final Specifications?*

   None.

2. *User assumptions?*

   None.

3. *Specific features of the codes used?*

   None.

ORNL

I. Primary system modelling

1. *Vessel thermal-hydraulic (T-H) model and nodalisation (1-D, 3-D and number of T-H channels or cells). How are the channels/T-H cells chosen?*

   Vessel is 3-D (18 channel code representation), loops and secondary side are 1-D. The T-H channels are chosen on the base of 60° symmetry in the VVER-1000 core.

2. *How the mixing is modelled?*

   Mixing is inherently taken into account with the 3-D reactor vessel model. No specific adjustment of the transverse junction loss factor was done.

3. *How are the lower plenum and downcomer modelled?*

   The lower plenum has three radial and three axial elements, the downcomer has eight axial and one radial nodes. They all have 60° symmetry in the horizontal plane.

4. *How are the upper head and the upper plenum modelled?*

   The upper plenum is modelled with three radial and three axial elements and the upper head has two axial and three radial nodes. A symmetry of 60° is respected again.

5. *How are the make-up and let-down system modelled and what is the logic used?*

   They are not modelled for this exercise.

6. *How are the pressuriser's heaters modelled?*

   Heaters do not operate during this test. The model exists but is not used.

7. *Are you using the pump head characteristics given in the specification?*

   Yes.

8. *Are using the MCP #3 rotor speed boundary conditions?*

   Yes.

II. Thermal-hydraulic core model

1. *Core thermal-hydraulic (T-H) model and nodalisation (1-D, 3-D and number of T-H channels or cells). How are the channels/T-H cells chosen?*

   The core is modelled with 18 hydraulic channels, representing 3 radial rings and azimuthal wedges.

2. *Number of heat structures (fuel rods) modelled?*

   Eighteen (18).

3. *What is the radial and axial heat structure (fuel rod) nodalisation?*

   Radial fuel temperature is calculated in 9 nodes, axially in 11 (10 active fuel).

4. *What is the relation used for Doppler temperature?*

   None.

5. *Used correlations for fuel properties vs. temperature?*

   Tabulated properties.

III. Secondary system

1. *Are you using steam generator (SG) feedwater boundary condition?*

   Yes.

2. *Are you using SG exit pressure boundary condition?*

   Turbine pressure BC is used.

IV. General

1. *Deviations from the updated Final Specifications?*

   None.

2. *User assumptions?*

   None.

3. *Specific features of the codes used?*

   None.

PSU

I. Primary system modelling

1. *Vessel thermal-hydraulic (T-H) model and nodalisation (1-D, 3-D and number of T-H channels or cells). How are the channels/T-H cells chosen?*

   The vessel is modelled in 3-D cylindrical geometry. The vessel model is subdivided into 20 axial layers, 5 radial rings, and 6 azimuthal sectors for a total of 600 T-H cells.

2. *How the mixing is modelled?*

   Mixing is taken into account with the 3-D reactor vessel model. By explicitly modelling the radial cross-flow between the T-H cells the code accounts for the mixing.

3. *How are the lower plenum and downcomer modelled?*

   Three-dimensional modelling.

4. *How are the upper head and the upper plenum modelled?*

   Three-dimensional modelling.

5. *How are the make-up and let-down system modelled and what is the logic used?*

   They were modelled according to the benchmark specification in such way to match the pressuriser liquid level and primary pressure.

6. *How are the pressuriser's heaters modelled?*

   They were modelled according to the benchmark Specification using the TRAC-PF1 heaters model in the pressuriser component.

7. *Are you using the pump head characteristics given in the specification?*

   Yes.

8. *Are using the MCP #3 rotor speed boundary conditions?*

   Yes.

II. Thermal-hydraulic core model

1. *Core thermal-hydraulic (T-H) model and nodalisation (1-D, 3-D and number of T-H channels or cells). How are the channels/T-H cells chosen?*

   The core is modelled in 3-D cylindrical geometry. The core model is subdivided into 10 axial layers, 3 radial rings and 6 azimuthal sectors for a total of 180 T-H cells.

2. *Number of heat structures (fuel rods) modelled?*

   Eighteen (18) rods in radial plane and 10 axial plane.

3. *What is the radial and axial heat structure (fuel rod) nodalisation?*

   Eight (8) radial and 100 axial nodes are used.

4. *What is the relation used for Doppler temperature?*

   As specified.

5. *Used correlations for fuel properties vs. temperature?*

   No.

III. Secondary system

1. *Are you using steam generator (SG) feedwater boundary condition?*

   Yes.

2. *Are you using SG exit pressure boundary condition?*

   Yes.

IV. General

1. *Deviations from the updated Final Specifications?*

   None.

2. *User assumptions?*

   None.

3. *Specific features of the codes used?*

   3-D vessel thermal-hydraulic capability.

UPISA

I. Primary system modelling

1. *Vessel thermal-hydraulic (T-H) model and nodalisation (1-D, 3-D and number of T-H channels or cells). How are the channels/T-H cells chosen?*

   Overall noding

   Four loops are modelled separately, each loop including hot legs, steam generators, main cooling pumps and cold legs. The pressuriser is connected with loop #4 via surge-line joining the bottom part of the hot leg. Relief valves are modelled on the top of the pressuriser. Control volumes are used to quickly achieve the steady-state conditions by adopting the "transient option". Control volumes can be isolated before the transient start to ensure that a stable dynamic condition is calculated by the code. The RPV is simulated using a 1-D model.

2. *How the mixing is modelled?*

   The mixing is considered homogeneous.

3. *How are the lower plenum and downcomer modelled?*

   The lower plenum is modelled as RELAP5 branch element, while a stack is used to simulate the downcomer region that extends till the bottom of the RPV to avoid the presence of nodes with stagnant flow. The downcomer stack is connected with cold legs.

4. *How are the upper head and the upper plenum modelled?*

   The upper plenum is modelled as a RELAP5 branch element, while the primary side of steam generators has been modelled by two vertical stacks of nodes simulating the hot and the cold header and by six groups of horizontal tubes. Within each group of horizontal tubes 19 subdivisions have been selected.

5. *How are the make-up and let-down system modelled and what is the logic used?*

   Not modelled.

6. *How are the pressuriser's heaters modelled?*

   Not modelled.

7. *Are you using the pump head characteristics given in the specification?*

   Yes.

8. *Are using the MCP #3 rotor speed boundary conditions?*

   Yes.

II. Thermal-hydraulic core model

1. *Core thermal-hydraulic (T-H) model and nodalisation (1-D, 3-D and number of T-H channels or cells). How are the channels/T-H cells chosen?*

   1-D model is used considering 28 heated parallel channel plus one bypass channel.

2. *Number of heat structures (fuel rods) modelled?*

   Twenty-eight (28).

3. *What is the radial and axial heat structure (fuel rod) nodalisation?*

   Twenty (20) axial nodes and 12 radial nodes.

4. *What is the relation used for Doppler temperature?*

   Constant coefficient.

5. *Used correlations for fuel properties vs. temperature?*

   No correlation are used, the properties are tabulated in function of the temperature.

III. Secondary system

1. *Are you using steam generator (SG) feedwater boundary condition?*

   Yes.

2. *Are you using SG exit pressure boundary condition?*

   No.

IV. General

1. *Deviations from the updated Final Specifications?*

   None.

2. *User assumptions?*

   None.

3. *Specific features of the codes used?*

   None.

OECD PUBLICATIONS, 2 rue André-Pascal, 75775 PARIS CEDEX 16
Printed in France.